Actinide Ground-State Properties

Theoretical predictions

John M. Wills and Olle Eriksson

For nearly fifty years, the actinides defied the efforts of solid-state theorists to understand their properties. These metals are among the most complex of the long-lived elements, and in the solid state, they display some of the most unusual behaviors of any series in the periodic table. Very low melting temperatures, large anisotropic thermal-expansion coefficients, very low symmetry crystal structures, many solid-to-solid phase transitions—the list is daunting. Where does one begin to put together an understanding of these elements?

In the last 10 years, together with our colleagues, we have made a breakthrough in calculating and understanding the ground-state, or lowest-energy, properties of the light actinides, especially their cohesive and structural properties. For all metals, including the light actinides, the conduction electrons produce the interatomic forces that bind the atoms together. In the light actinides, it is the s, p, and d valence electrons and also the 5f valence electrons that contribute to chemical bonding (binding). When they are valence electrons in isolated atoms, the 5f electrons have an orbital angular momentum $\ell = 3$, and they orbit around the atomic nuclei at speeds approaching the speed of light. In the solid, these electrons are thought to be at least partially shared by all the atoms in the crystal. Therefore, they are thought to be participating in bonding. Moreover, their relativistic motion and their electron-electron correlations—the interactions among the 5f electrons and between them and other electrons—are expected to affect the bonding.

Low-symmetry crystal structures, relativistic effects, and electron-electron correlations are very difficult to treat in traditional electronic-structure calculations of metals and, until the last decade, were outside the realm of computational ability. And yet, it is essential to treat these effects properly in order to understand the physics of the actinides. Electron-electron correlations are important in determining the degree to which 5f electrons are localized at lattice sites. If they are localized, the 5f electrons are atomic-like and do not contribute to bonding; if they are not localized, they are itinerant, or conducting, and contribute to bonding. Many of the fundamental properties of the actinides hinge on the properties of the 5f electrons and on the question of whether those electrons are localized or delocalized.

During the past 10 to 15 years, however, there has been a minirevolution in electronic-structure calculations. It has become possible to calculate from first principles (that is, without experimental input) and with high accuracy the total ground-state energy of the most complicated solids, including the actinides. Density functional theory, or DFT (Hohenber and Kohn 1964, Kohn and Sham 1965), the variational formulation of the electronic-structure problem, enabled this accomplishment. DFT gives a rigorous description of the total electronic energy of the ground state of solids, molecules, and atoms as a functional of electron density. The DFT prescription has had such a profound impact on basic research in both chemistry and solid-state physics that Walter Kohn, its main inventor, was one of the recipients of the 1998 Nobel Prize in Chemistry.

In general, it is not possible to apply DFT without some approximation. But many man-years of intense research have yielded reliable approximate expressions for the total energy in which all terms, except for a single-particle kinetic-energy term, can be written as a functional of the local electron density. Even the complicated electron-electron exchange term arising from the Pauli exclusion principle and the electron-electron electrostatic interactions can be approximated in this way. Called the local density approximation, or LDA, this development has yielded more accurate results than anyone ever dreamed possible. We have developed bases, algorithms, and software to perform the calculation efficiently and accurately.[1] The efficiency allows us to get solutions for arbitrary geometries, including low crystal symmetry and complex unit cells, and to vary the inputs and thereby investigate the trends and the microscopic mechanisms behind the chemical bonding of solids. Once we know the total energy,

[1] One of the most reliable and robust theoretical methods and software packages for performing such calculations is the FP-LMTO software package developed by John Wills at Los Alamos.

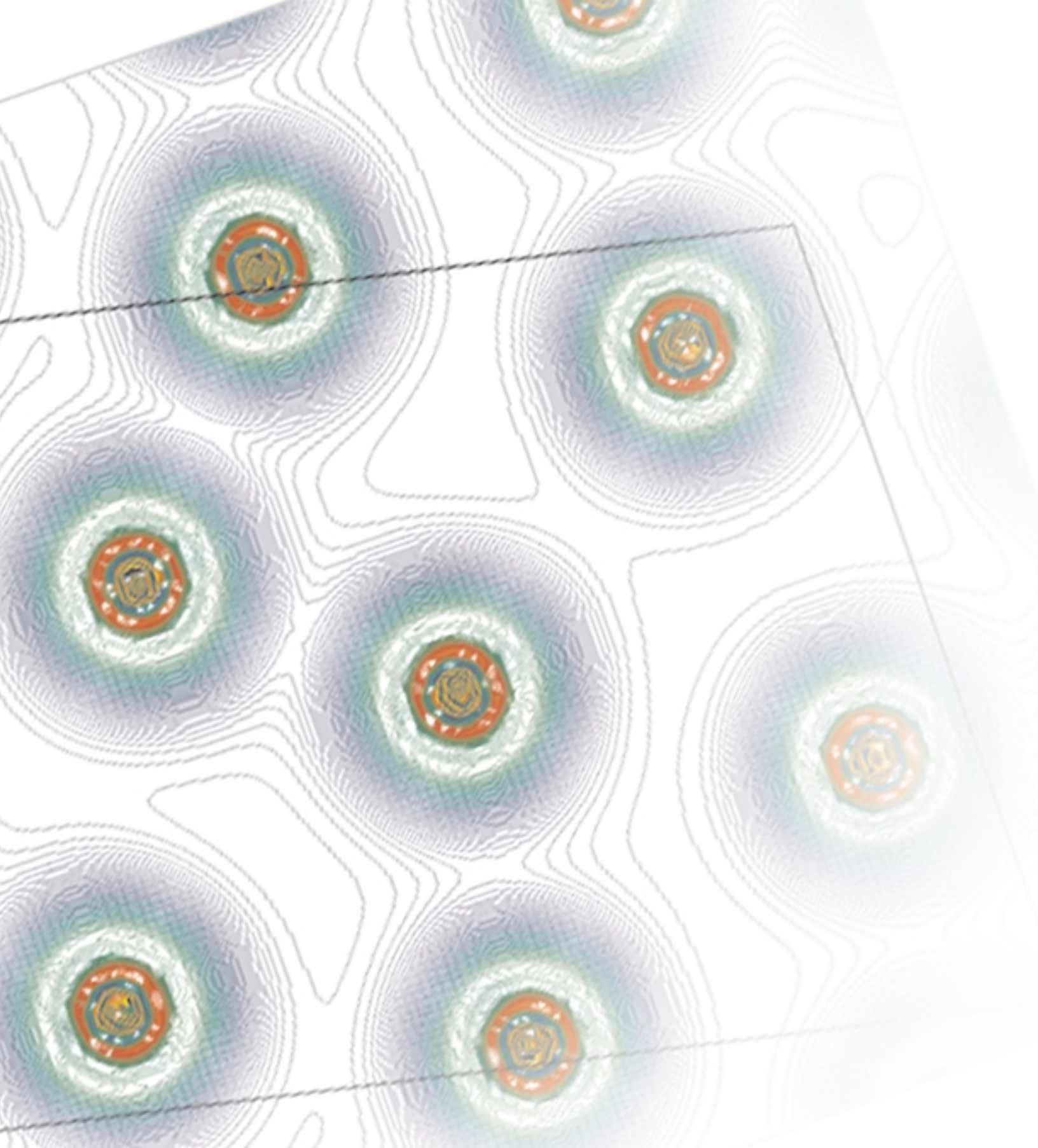

We calculated this contour plot of electron density for α-plutonium from first principles by using density functional theory. The parallelepiped outlines the 16-atom simple monoclinic unit cell. The contours show more charge buildup away from the bonds, indicating that covalent bonding is not prevalent in α-plutonium.

nisms behind the chemical bonding of solids. Once we know the total energy, we can easily calculate all the quantities related to the energy as a function of position, such as pressures and interatomic forces. Our calculations are highly accurate and often predictive.

In this article, we present our calculations of the light actinides (thorium through plutonium) in their observed low-symmetry structures. We have developed a firm theoretical understanding of the equilibrium volume, structural stability, cohesive energy, and magnetic properties of these elements at $T = 0$. We have been able to reproduce the observed lattice constants of the light actinides to within about 5 percent, to determine structural stabilities—including pressure-induced phase transitions—that agree well with experiment, to predict high-pressure structural phase transitions, and to reproduce magnetic susceptibilities that agree with observations. We have also developed a modified version of our methodology that describes with some accuracy the δ-phase of plutonium, that is, the face-centered-cubic (fcc) phase of the metal used in nuclear weapons. Perhaps more important than the numerical results is a new understanding about why the actinides form in the structures in which they do. In particular, our results contradict the old adage that the low-symmetry crystal structures of the actinides are a consequence of the directional character of the 5f spherical harmonic functions.

The success of DFT in reproducing and sometimes even predicting the ground-state properties of the actinides suggests that accurate computer simulations of the properties of other materials might become feasible. In the concluding section, we discuss the possibility of simulating defect formation, grain boundaries, segregation of specific atomic impurities in plutonium to the surface or to grain boundaries, and alloy formation. From the point of view of stockpile stewardship, simulating the material properties of the actinides would, of course, be valuable.

Background to the Modern Developments

Despite the brilliant accomplishment of nuclear physics in predicting the existence of plutonium and its fission properties and then creating this new material, it took a long time before the chemistry of element 94 was understood well enough to enable scientists to place plutonium in the periodic table. It was initially speculated that plutonium and the other light actinides—actinium, thorium, protactinium, uranium, and neptunium—were the early part of a 6d transition metal series in analogy with the 3d, 4d, and 5d transition metal series. That is, an increase in the atomic number of the element would correspond to an increase in the number of electrons in the 6d electronic shell. For this reason, the manmade element with atomic number 94 was initially named eka-osmium and was expected to have the same valence configuration and thus the same chemical properties as osmium. Then, Seaborg suggested (1945) that the elements from actinium through plutonium were the early part of a new series called "the actinide series." In this series, by analogy with the lanthanide series, the f rather than the d shell was being filled. The 4f electrons in the lanthanides tend to be localized at lattice sites; in other words, they are chemically inert and do not contribute to the cohesion of the solid. Hence, the electronic bonding for the lanthanides is provided by three (and sometimes only two) conduction-band electrons.

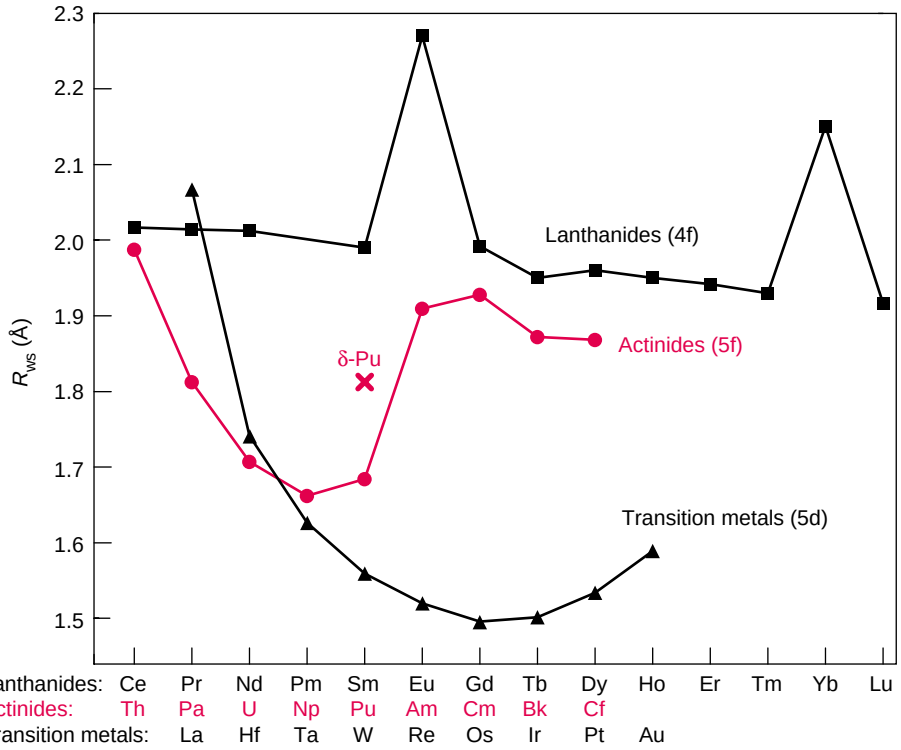

Figure 1. Experimental Wigner-Seitz Radius of Actinides, Lanthanides, and Transition Metals

The Wigner-Seitz radius R_{WS} (the radius of the volume per atom in a solid) is defined as $(4\pi/3)R_{WS}^3 = V$, where V is the equilibrium volume of the primitive unit cell. The atoms of the actinides, lanthanides, and transition metals are aligned so that elements that lie on top of each other have the same number of valence electrons. The volumes of the light actinides and the light transition metals decrease with increasing atomic number, whereas the volumes of the lanthanides remain about constant. For that reason, it was originally thought that the light actinides were the beginning of a 6d transition-metal series.

Figure 1 compares the experimental equilibrium volumes of the lanthanides and actinides with those of the 5d transition metals. From this figure, it is easy to see why it was tempting to think of the light actinides as a d transition series rather than an f series. The equilibrium volumes are similar for the transition metals and the light actinides, decreasing parabolically as a function of increasing atomic number, which indicates that the valence electrons in the light actinides contribute to bonding.

The first calculations of the electronic structure of the actinides, which were made almost three decades ago (Kmetko and Waber 1965, Hill and Kmetko 1970, Koelling et al. 1970), finally resolved questions about the nature of the chemical bonding in the light actinides and about the role played by the 5f electrons. Those calculations showed that the 5f electrons do not have sharp energies characteristic of atomic-like energy levels. Instead, they occupy a band of energy levels whose energy spread is 3 to 4 electron volts (eV). Occupancy in an energy band signifies that the 5f electrons are not localized at lattice sites but are itinerant and, hence, chemically active in binding the solid together. As we will outline later, the Friedel model (Friedel 1969), which is a simplified model of bonding by conduction electrons, has successfully explained the equilibrium volumes of both the transition metals and the light actinides. Thus, the nature of the chemical bonding appears to be similar in both series of elements.

A closer examination of the ground states shows some important differences between these different series. First, the parabolic dependence in the equilibrium volumes of the actinides ends abruptly between plutonium and americium. Second, the transition metals and actinides differ in their low-temperature crystal structures. The transition metals[2] form in close-packed, high-symmetry

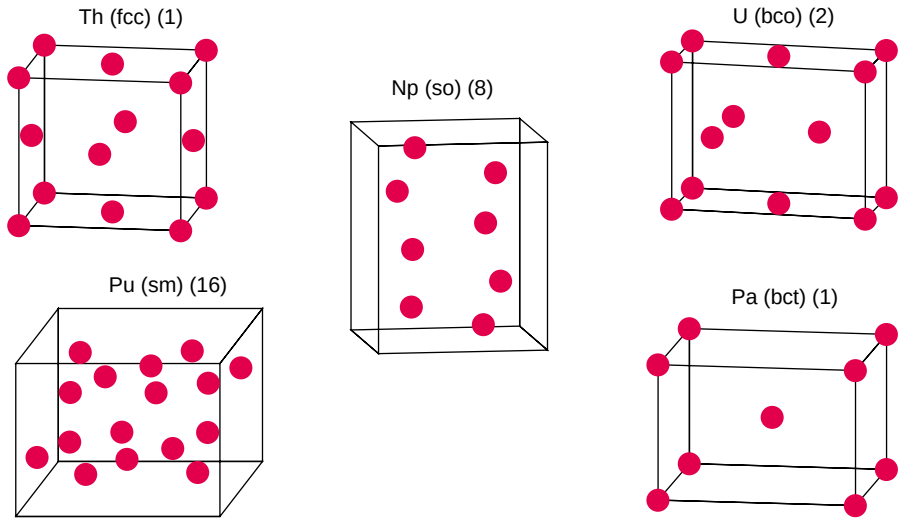

Figure 2. Experimental Crystal Structures of the Light Actinides

Illustrated here are the conventional unit cells of the ground-state crystal structures of the light actinides (thorium through plutonium). The number in parentheses represents the number of atoms in the primitive cell. Notice that most of these structures are open in contrast to the close-packed hcp, fcc, and bcc structures of the transition metals.

structures, such as hexagonal close-packed (hcp), face-centered cubic (fcc), and body-centered cubic (bcc), whereas the light actinides form at low temperatures in the low-symmetry, open-packed structures shown in Figure 2. For instance, protactinium forms in a body-centered-tetragonal (bct) structure, and uranium and neptunium form in orthorhombic structures with 2 and 8 atoms per cell, respectively. At low temperatures, plutonium forms in a monoclinic structure with 16 atoms per cell. Of all the actinide metals, plutonium shows by far the most complex structural properties. Given the similarities between the transition metals and the light actinides regarding equilibrium volumes and chemical bonding, one may ask why the two series are so different in structural properties. Below, we will explain the origin of this difference.

Figure 1 also shows that the equilibrium volumes of the actinides past plutonium resemble those of the lanthanides, remaining relatively constant as a function of atomic number. The usual explanation is that, like the 4f electrons in the lanthanides, the 5f electrons in the heavy actinides become localized, or atomic-like, through a Mott transition (Skriver et al. 1978, Skriver et al. 1980, Brooks et al. 1984). In this picture, localization occurs because 5f (or 4f) electron-electron correlations at a given lattice site become large enough to prevent those electrons from hopping between sites. This phenomenon has actually motivated some scientists to call the heavy actinides a second rare-earth series. It is interesting to note that the famous isostructural expansion in cerium from the alpha to the gamma phase appears to be a Mott transition, in which strong correlations at lattice sites cause the electrons in the $4f^1$ conduction band to become localized (Johansson 1974).

The δ-phase of plutonium, the fcc phase that is malleable and therefore of interest for nuclear weapons, is stabilized at room temperature by the addition of, for instance, a few percent atomic weight of gallium. In this phase, plutonium appears to be different from the light and heavy actinides. Figure 1 shows that the equilibrium volume of δ-plutonium is between that of α-plutonium and americium. Electron-electron

[2] Manganese, which has a very complex crystallographic and magnetic structure, is an exception to this rule.

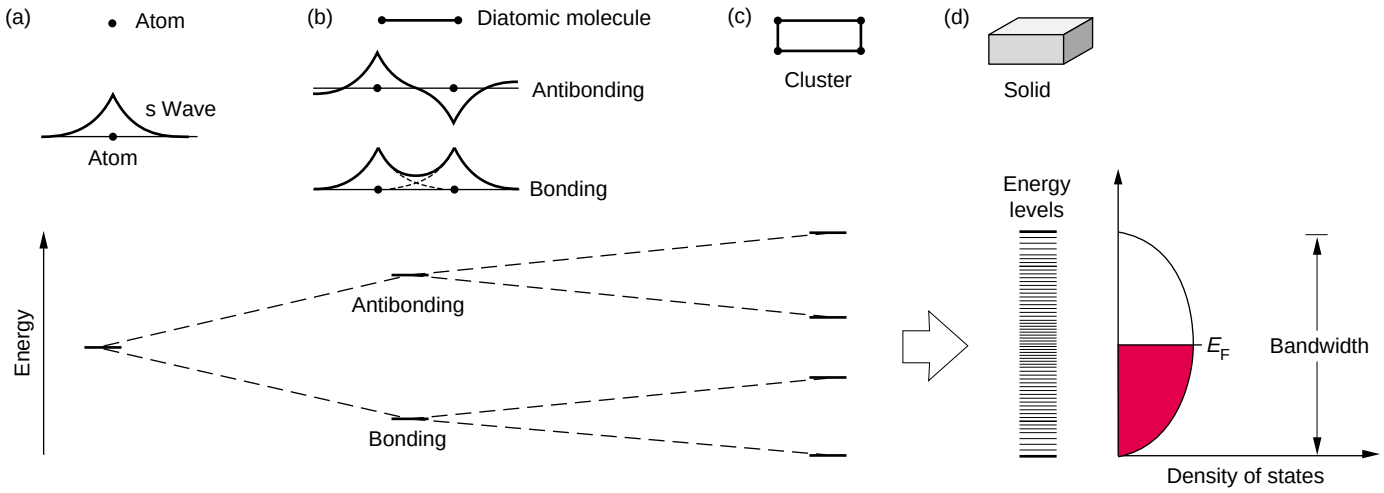

Figure 3. Formation of Energy Bands in Solids

(a) Shown here are the radial wave function and the energy level for a 1s valence electron in an isolated atom. (b) When two such atoms are brought together, their s-electron wave functions will hybridize to form the bonding and antibonding orbitals of a diatomic molecule. The bonding orbital is the sum of the two atomic wave functions, whereas the antibonding orbital is the difference between them. The original energy level has split into two: The lower level is the energy of the bonding orbital, and the upper, the energy of the antibonding orbital. As shown in (c), the energy levels split again when four atoms are brought together to form a cluster, and again they correspond to bonding and antibonding states. When a very large number of atoms are brought together into a solid (d), their energy levels form a closely spaced band corresponding to both the bonding and the antibonding states. Note that the width of the energy band is about equal to the difference between the bonding and antibonding energy levels in the diatomic molecule. The levels in the energy band are so tightly packed that we consider the one-electron energy e to be a continuous variable and enumerate the levels in terms of a density of states function $D(e)$. The shaded region of $D(e)$ represents the occupied levels at $T = 0$, that is, all levels are occupied up to the Fermi level, E_F.

correlations are apparently very important in this phase and produce a nonmagnetic state, in which the electrons are neither fully localized nor fully delocalized. Thus, the electronic configuration of δ-plutonium may be unique among the configurations of the other elements in the periodic table.

At the end of this paper, we review our recent attempt (Eriksson et al. 1999) at describing the δ-phase and demonstrate that a specific approximation to DFT reproduces the equilibrium volume, energy, and elastic properties of this unusual state. Our approach is based on the model of electron-electron correlations associated with a Mott transition. That is, some of the f electrons in plutonium localize at lattice sites through very strong correlations. This localization occurs in a bath of spd conduction electrons, ensuring metallic behavior on both sides of the transition (Johansson 1974, Skriver et al. 1978, Skriver et al. 1980, Brooks et al. 1984). Is this a correct description of the electron correlations in plutonium? This question is very much open to investigation. Other attempts at describing the electron correlations in plutonium might include the following: the GW approximation, which uses a Green's function approach and a screened Coulomb interaction (Hedin 1965), a perturbation series in the occupation fluctuation (Steiner et al. 1992), the dynamical mean-field theory (Georges et al. 1996), and an ab initio treatment of the Anderson model, which includes strong electron correlations (Sandalov et al. 1995).

Energy Bands in Metals

Just as the energy levels and the corresponding electron states (atomic orbitals) provide a fundamental basis for understanding and predicting the properties of atoms, the allowed states of the conduction electrons provide a basis for understanding most properties unique to metals. In the one-electron theory of metals, the allowed states of conduction electrons are single-particle wave functions spread throughout the crystal, and the allowed energies of

those itinerant electrons are grouped into sets of very closely spaced energy levels referred to as energy bands. At $T = 0$, the states within an energy band are occupied by electrons in increasing order of energy, and in a metal, there are only enough valence electrons to partially fill the conduction band. The highest occupied energy level (called the Fermi level, E_F) is defined in such a way that the number of energy levels below E_F is equal to the number of electrons.

Although energy bands are not rigorously meaningful in the DFT approach, we can obtain an often-useful approximation to the physical spectrum from our solution for the total energy and charge density. In fact, whenever we seek to understand the physical mechanisms behind our density functional results on structural stability and other properties, we return to the energy bands and examine their behavior.

Formation of Energy Bands. One may think of how an energy band is formed in the following simple terms. Consider an atom with its discrete spectrum of single-electron energy levels, for instance, of s angular character (the orbital angular momentum is $\ell = 0$). Figure 3(a) shows the energy level and the radial shape of the s electron wave function. If two such atoms are brought together to form a diatomic molecule—Figure3(b)—the s electron wave functions of each atom will overlap and combine, or hybridize, to form two new states: the bonding and antibonding wave functions of the diatomic molecule. The bonding state is the sum of the two atomic s wave functions, whereas the antibonding state is the difference between those wave functions. In this simplified model, the energy of the bonding state is $E_{\text{bond}} = E_{\text{atom}} - h$, and the energy of the antibonding state is $E_{\text{anti}} = E_{\text{atom}} + h$, where h is the magnitude of the integral between the wave functions ψ on the two sites (A and B) and the potential V. In other words, $h = |(\psi_A|V|\psi_B)|$. The closer the atoms or the larger the overlap between the atomic wave functions, the bigger is the hybridization parameter h, and the larger is the energy difference between the bonding and antibonding states. The lowered state is called a bonding state because occupying it lowers the energy and stabilizes the system; the raised state is called an antibonding state because occupying it raises the energy and destabilizes the system.

Figure 3(c–d) shows that a similar pattern ensues if more atoms are brought together to form a cluster of atoms. The number of energy levels increases, and the levels divide into a set of bonding states and a set of antibonding states. Finally, if very large numbers of atoms are brought together into a solid, the atomic levels evolve into a band of closely spaced energy levels containing both bonding and antibonding states. Although the set of energy levels remains discrete, the number of levels in the band is so large (on the order of 10^{23}) and the spacing between levels so small that it is more useful to consider the energy as a continuous variable and to enumerate the electron energy levels (states) in terms of a density of states at a given energy.

The width of the energy band in a metal can be related to the energy levels of the diatomic molecule. Just as in the case of two atoms, the smaller the interatomic distance, the larger the overlap of the electron wave functions and the wider the spread in energies from the top to the bottom of the energy band. Notice also that, if the bonding electron states were the only states occupied, reducing the interatomic distance would, according to the discussion above, always lower the total energy and lead to an infinitely contracted lattice or molecule. But the total energy of the solid is not equal to the sum of energies shown in Figure 3. Other terms, such as the electrostatic Hartree term—see Equation (9) in the box "Basics of the DFT Approach"—balance the band-formation term, preventing the molecule or solid from collapsing. For those readers familiar with second quantization, we include the box "A Model Hamiltonian for Conduction Electrons," which presents a particle picture (as opposed to a wave picture) of the essential physics of band formation in an analytically solvable form.

The actinides do not have just one energy band. Instead, they have a set of bands, each typically labeled by the orbital quantum numbers (s, p, d, or f) of the atomic valence state from which the band originated. However, angular momentum is ill-defined for a conduction electron moving through the lattice, and so the energy bands that overlap in energy tend to lose their original identity and behave as a single energy band, especially when the bands are broad.

In calculating these conduction bands, one can usually neglect the effects of the surface and treat the solid as if it had periodic boundary conditions and as if its extent were infinite. The atoms in this idealized solid are arrayed on a perfect crystalline lattice (also called a Bravais lattice), with lattice vectors $\boldsymbol{R}$. Because the crystal looks the same from any lattice site (that is, it is translationally invariant), the wave function of an electron can only differ by a phase $e^{i\boldsymbol{k}\cdot\boldsymbol{R}}$ from one periodic cell to the next. The wave vector $\boldsymbol{k}$ must lie within the unit cell of the lattice reciprocal to the Bravais lattice (the unit cell is equivalent to the Brillouin zone). For that reason, the electron states (also known as the Bloch states) in a crystal are characterized by the modulation vector $\boldsymbol{k}$, and the energy levels in an energy band are described by a function of the wave vector $e(\boldsymbol{k})$.[3]

The wave vector $\boldsymbol{k}$ is often called the electron's crystal momentum because it enters conservation laws that are analo-

[3] When the atoms in the solid are arrayed on a crystalline (Bravais) lattice, electron states are representations of the (Abelian) translation group and, hence, can acquire a phase $e^{i\boldsymbol{k}\cdot\boldsymbol{R}}$ on being translated by lattice vectors $\boldsymbol{R}$, with $\boldsymbol{k}$ lying in the unit cell of the lattice reciprocal to the Bravais lattice. We thus arrive at the conventional description of the energy of an electron in a crystal $e(\boldsymbol{k})$, which is a function of the translation quantum number, or crystal momentum $\boldsymbol{k}$.

A Model Hamiltonian for Conduction Electrons

One can think of conduction electrons as waves traveling through the crystal, but one can also think of them as particles hopping from one lattice site to the next. The model Hamiltonian in Equation (1) embodies this particle picture.

$$H = e\sum_i \hat{n}_i + h\sum_i \sum_{i' \neq i} \hat{c}_{i'}^{\dagger}\hat{c}_i \quad , \tag{1}$$

where $\hat{c}_i^{\dagger}$ $(\hat{c}_i)$ is the creation (destruction) operator for site i and $\hat{n}_i = \hat{c}_i^{\dagger}\hat{c}_i$ is the number operator for site i.

This Hamiltonian describes a set of N valence electrons from N neutral atoms that have condensed into a solid and are located at lattice sites i. The electrons in their atomic state have only one degenerate energy level with energy e. The first term in the Hamiltonian contains the number operator $\hat{n}_i$, which counts the number of electrons at site i. Thus, the first term is the sum of the energies of all the electrons located at lattice sites. The second term contains the creation operator $\hat{c}_{i'}^{\dagger}$, which creates an electron at site i', and the annihilation operator $\hat{c}_i$, which annihilates an electron at site i. Thus, the second term in the Hamiltonian causes an electron to jump from site i to site i'. The likelihood of that jump is proportional to h, the hopping strength, or hybridization strength (we take h to be non-negative).

This Hamiltonian is interesting because it is simple enough to solve analytically, and yet it captures the most important aspects of the interactions in the system—in particular, the formation of energy bands. For example, suppose $N = 2$ so that only two such atoms are brought in proximity. If one solves for the energy levels of this model two-atom system (by diagonalizing a 2×2 matrix), one finds that the single energy level e will split into a bonding level $e - h$ and an antibonding level $e + h$. If many such atoms are brought together to form a solid, the atomic levels evolve into a set of levels falling approximately in the range spanned by a simple, two-atom bonding-antibonding picture. The eigenstates (electron wave functions) of this Hamiltonian are itinerant—that is, their density is spread among all the atoms of the system. When the atoms are far apart and the atomic wave functions barely overlap, h in Equation (1) is small, and the energy levels fall into a narrow range. In this case, the eigenstates, though itinerant, retain much of the character of the atomic states from which they evolve and are usually (and loosely) labeled by the atomic orbital quantum number from which they evolve (s, p, d, or f). As the atoms are brought still closer together, the strength of the hybridization potential—h in Equation (1)—increases, the range of energy levels broadens, and the electronic states lose much of their atomic character and become, in essence (though not in detail), free-electron-like.

In the section describing the Mott transition in the actinide elements, we will show how correlation effects can be added to the model Hamiltonian of Equation (1).

gous to the momentum conservation law for free particles. In contrast to the orbital labels (s, p, d, and f), the crystal momentum is a true quantum number of electrons in a perfect periodic lattice. For narrow bands, however, whose electrons can be thought of as partially localized, the orbital labels inherited from atomic orbitals are useful and meaningful characterizations.

Density Functional Theory (DFT)

The general features of energy bands and the reasons for their existence are not difficult to grasp, but solving the equations for the bands is complicated. For many decades, band calculations were limited to the simplest crystal structures with unit cells containing only one or two atoms and with spherically symmetric potentials around each atom. In the absence of a total energy functional of DFT, the cohesive energy of a solid could not be calculated with any degree of accuracy. Instead, one focused on determining the dispersion curves for the energy bands $e(\boldsymbol{k})$ and the shape of the Fermi surface, which is just the portion of $\boldsymbol{k}$-space occupied by electrons at the Fermi energy level, E_F.

As we mentioned in the introduction, the application of DFT has led to a tremendous simplification of band structure calculations. In its pure form, DFT outlines a rigorous prescription for calculating the total electronic energy of solids, molecules, and atoms in the ground state (at $T = 0$) in terms of a functional of the total charge density. In most practical applications, however, one can get excellent results by using local functions of the density to express the entire DFT energy functional, including the usual nonlocal exchange and correlation terms. The LDA approximates the exchange and correlation term as a local function of density, and the general gradient approximation, or GGA, expresses that term as a local function of density and density gradient. Because of this simplification, calculating the total energy of an electronic system becomes possible. The box on the next page briefly outlines the mathematical framework of density functional calculations.

We must also note that most implementations of DFT have a strong connection to energy band theory in the form used before DFT was invented. As a matter of fact, the Kohn-Sham equation, the crucial equation normally

continued on page 138

Basics of the Density Functional Theory (DFT) Approach

To calculate the ground-state electronic energy of an atomic system, one normally starts from the time-independent Schrödinger equation. In addition, the Born-Oppenheimer approximation is frequently used because it neglects the motion of the nuclei and allows calculating the total energy of the electrons in the potential created by the nuclei. Therefore, one could calculate the ground-state (lowest-energy configuration) total electronic energy from

$$H\,\Psi(r_1, r_2, \ldots r_n) = E\,\Psi(r_1, r_2, \ldots r_n) \quad , \tag{2}$$

where H is the Hamiltonian containing the kinetic energy and all the interactions of the system (electron-electron correlation and exchange and electron-nuclei interactions), $\Psi(r_1,r_2,\ldots r_n)$ is a many-electron wave function of the n-electron system, and E is the total electron energy of the ground state. The input parameters in Equation (2) are the atomic numbers of the atoms and the geometry of the crystal (the lattice constant, the crystal structure, and the atomic positions).

To determine the equilibrium volume theoretically, one could keep the crystal structure fixed and calculate the ground-state electronic energy for different input volumes (or lattice constants). The volume that produced the lowest energy would represent the theoretical equilibrium volume. Similarly, one could compare the total energy of different structures at different volumes and draw conclusions about structural stability and possible structural phase transitions that might occur when the volume is changed (experimentally, one can compress the volume by applying an external pressure). In addition, one could calculate the energy gain when free atoms condense to a solid (the cohesive energy). Unfortunately, there is no practical way to solve Equation (2) for a solid.

Nevertheless, we have been able to carry out this program of calculations because there is an alternative theoretical formulation for determining the electronic structure. In two important theorems (Hohenberg and Kohn 1964, Kohn and Sham 1965, Dreitzler and Gross 1990), it has been shown that the total energy of a solid (or atom) may be expressed uniquely as a functional of the electron density. We can therefore minimize this functional with respect to the density in order to determine the ground-state energy. Therefore, instead of working with a many-electron wave function, $\Psi(r_1,r_2,\ldots r_n)$, one can express the ground-state energy in terms of the electron density at a single point n(r), where that density is due to all the electrons in the solid:

$$n(r) = \sum_{i=1}^{n} \int \Psi^{*}(r_1, r_2, \ldots r_n)\,\delta(r - r_i)\,\Psi(r_1, r_2, \ldots r_n)\,dr_1 dr_2 \cdots dr_n \quad , \tag{3}$$

In addition, Hohenberg and Kohn (1964), Kohn and Sham (1965), and Dreitzler and Gross (1990) demonstrated that, instead of calculating the electron density from the many-electron wave function $\Psi(r_1,r_2,\ldots r_n)$, one may work with the solutions to an effective one-electron problem.

The trick is to use the form of the total-energy functional to identify an effective potential V_{eff}(r) for one-electron states and then solve for the one-electron states to produce a density equal to the many-electron density. The equation for the one-electron states is

$$\left(\hat{T} + V_{\text{eff}}\right)\psi_i(r) = e_i\,\psi_i(r) \quad , \tag{4}$$

where $\hat{T}$ is a kinetic energy operator (for example, $-\hbar^2\nabla^2/2m$ in a nonrelativistic approximation)

and the resulting total electron density is given by

$$n(r) = \sum_i \left|\psi_i(r)\right|^2 \quad . \tag{5}$$

To include relativistic effects important in the actinides, one replaces the nonrelativistic, Schrödinger-like one-electron equation—see Equation (4)—by the relativistic Dirac equation. By finding the correct form for the effective potential, the electron density in Equation (5) will be the same as that in Equation (3).

As mentioned in the section “Density Functional Theory” in the main text, the one-electron problem defined by Equation (4) has the same form as the equations solved by band theorists before DFT was invented, and the eigenvalues of those equations as a function of crystal momentum are precisely the energy bands. The contribution of DFT is to provide a rigorous prescription for determining the effective potential and for calculating the total ground-state energy. The DFT prescription for the effective potential in Equation (4) is

$$V_{\text{eff}}(r) = \frac{\delta}{\delta n(r)}\left[E_H(n(r)) + E_{xc}(n(r)) + E_{eN}(n(r))\right] \quad , \tag{6}$$

where the different terms are derived from the total-energy functional $E(n(r))$:

$$E(n(r)) = T(n(r)) + E_H(n(r)) + E_{xc}(n(r)) + E_{eN}(n(r)) + E_{NN} \quad . \tag{7}$$

In this equation, $T(n(r))$ represents the kinetic energy of the effective one-electron states and is calculated from

$$T(n(r)) = \sum_i \int \psi_i^{\dagger}(r)\,\hat{T}\,\psi_i(r)\,dr \quad . \tag{8}$$

$E_H(n(r))$ is the classical Hartree interaction (the electrostatic interaction between two charge clouds):

$$E_H(n(r)) = \frac{1}{2}e^2 \int \frac{n(r_1)n(r_2)}{|r_1 - r_2|}\,dr_1 dr_2 \quad . \tag{9}$$

$E_{eN}(n(r))$ is the electron-nuclei interaction:

$$E_{eN}(n(r)) = -e^2 \sum_R Z_R \int \frac{n(r)}{|r - R|}\,dr \quad . \tag{10}$$

$E_{xc}(n(r))$ is the part of the interaction that goes beyond the classical Hartree term as well as the difference between the true kinetic energy and the one-electron kinetic energy. In the LDA, this term has the form

$$E_{xc}(n(r)) = \int n(r)\,\varepsilon_{xc}(n(r))\,dr \quad . \tag{11}$$

Finally, E_{NN} is the Coulomb interaction between the different atomic nuclei of the lattice:

$$E_{NN} = \frac{1}{2}e^2 \sum_R \sum_{R' \neq R} \frac{Z_R Z_{R'}}{|R - R'|} \quad . \tag{12}$$

From these definitions, it becomes obvious that the effective potential in which the electron moves has contributions from the electron's interaction with the nuclei and the other electrons in the solid both by the classical Hartree term and by the quantum mechanical exchange and correlation term.

Because all electron-electron interactions that go beyond the classical Hartree term are found in $E_{XC}(n(r))$, it is crucial to have a good approximation for this term (unfortunately, there is no exact form of this term for a real solid). However, if one assumes the functional to be local, a numerical form may be obtained from many-body calculations (quantum Monte Carlo or perturbation series expansion), and very good values may be obtained for the ground-state energy for different values of the electron density. If the electron density of a real system varies only smoothly in space, one expects that a form of E_{XC} taken from a uniform electron gas should be applicable to the real system as well. This approximation is no other than the LDA. The good agreement, for many solids,* on cohesive energy, equilibrium volume, and structural properties between this approximate theoretical approach and experimental values suggests that the LDA form of E_{XC} works even if the electron density varies rapidly in space. As an example of how E_{XC} might look, we quote the full form of the exchange and correlation energy density in Equation (11), as given by Hedin and Lundqvist, with parameters calculated in the random-phase approximation:

$$\varepsilon_{xc}(n(r)) = \varepsilon_x(r_s) + \varepsilon_c(r_s) \quad ,$$

where

$$r_s = \left(\frac{3}{4\pi n(r)}\right)^{\frac{1}{3}}$$

$$\varepsilon_x(r_s) = \frac{-0.91633}{r_s}$$

$$\varepsilon_c(r_s) = -0.045\, G\left(\frac{r_s}{21}\right)$$

$$G(x) = (1+x^3)\ln\left(1+\frac{1}{x}\right) - x^2 + \frac{x}{2} - \frac{1}{3} \quad . \qquad (13)$$

Thus, one can calculate the total ground-state energy by solving an effective one-electron equation. This tremendous simplification of replacing interacting electrons with effective one-electron states will work only if one can find the correct, effective one-electron potential. ■

*Among such solids are simple metals, transition metals, actinides, p electron elements, and thousands of compounds formed between these elements.

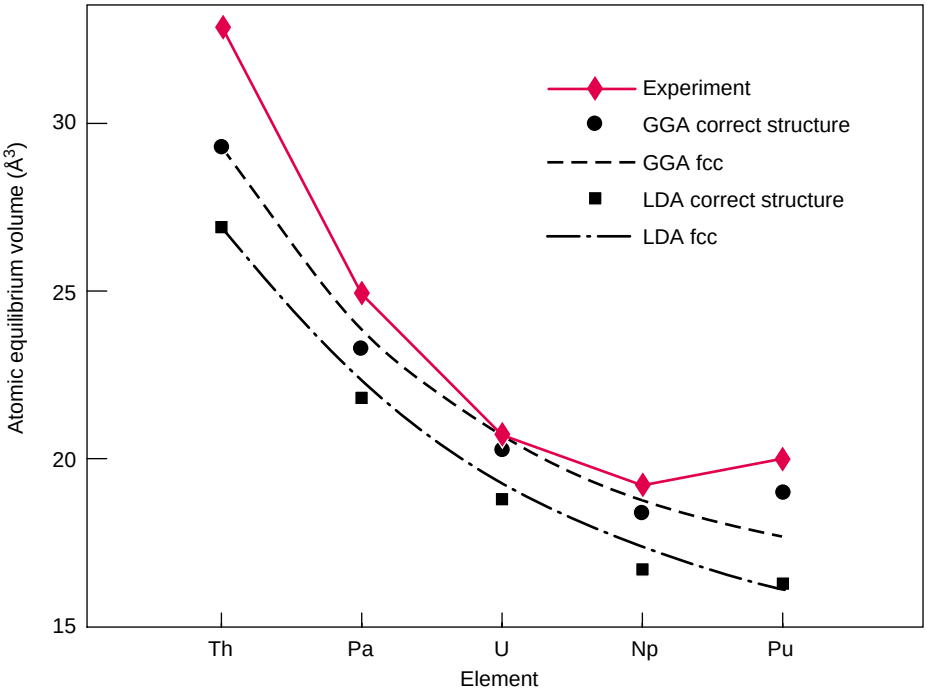

Figure 4. DFT and Experimental Equilibrium Volumes for the Light Actinides
We used DFT to compute the equilibrium volume of each light actinide in its observed crystal structure and in a hypothetical fcc structure. In each calculation, we used first the local density approximation (LDA) and then the generalized gradient approximation (GGA). Our LDA values are systematically smaller than the experimental ones, but the GGA results are typically a few percent larger and in better agreement with observation. In fact, our GGA calculations reproduce some of the finer details of the observations, including the small increase in equilibrium volume between α-neptunium and α-plutonium. This result implies that the 5f electrons in α-plutonium, like the 5f electrons in α-uranium, are delocalized.

continued from page 134

solved in DFT, is identical in form to the one solved by the Slater X-α method, as is any one-electron-like equation. In addition, the exchange part of the effective potential is very similar in the two methods. Unlike traditional approaches, however, DFT derives its strength from the fact that it gives an explicit and well-founded form for the total energy of the electrons in the lattice in terms of a functional of the total electron density. Hence, DFT could be said to have two outputs: first, and most important, the total energy and charge density of the electrons in the solid and second (and less rigorously comparable to experiment), the energy bands and density of states. The latter set of properties can also be calculated from band theory with the Slater X-α method.

Equilibrium Volumes from DFT Calculations. In Figure 4, we display the calculated equilibrium volumes of all the light actinides for several different inputs in order to show the results from the DFT energy functional defined in Equation (7). We used both the observed crystal structure as well as a hypothetical fcc structure for each element (for thorium, the observed structure is fcc). We then repeated the calculation using the two most common approximate forms for the DFT energy functional, the LDA and GGA. These two approximations designate specific forms of the exchange and correlation term E_{xc} shown in Equations (11) and (13). In the LDA, E_{xc} is a local function of density; in the GGA, it is a local function of density and density gradient.

Notice that, without any experimental information, one can reproduce the observed equilibrium volumes with good accuracy. Our LDA-calculated values for the volumes of the actinides are systematically smaller than the experimental values. This shortcoming is true for most materials, but it can be corrected if we use the GGA, which normally gives equilibrium volumes that are a few percent larger.

Considering the approximations that enter practical calculations, we expect some disagreement between theory and experiment. But the real power of these types of calculations is not the accurate reproduction of experimental data to within the second or third decimal point but the ability to identify the physical mechanisms underlying the general trends in cohesion, magnetism, superconductivity, or any other phenomenon one is interested in. Having said this, we note that our present calculational scheme reproduces the finer details of the observations, including the small increase in volume between α-neptunium and α-plutonium. This result is important because it implies that the 5f electrons in α-plutonium are delocalized in much the same way as the 5f electrons in α-uranium. Before our calculations, that point was a matter of some controversy.

The one-electron energies from Equation (4), or the energy bands $e(\boldsymbol{k})$, are another output from the DFT prescription. Figure 5 displays our DFT results for the energy bands in α-uranium. The figure also shows the density of states as a function of energy that results from the α-uranium band structure and the calculated Fermi energy E_F for this metal.

The Friedel Model

The calculated density of states in Figure 5 is very complicated, and often one wants to estimate various metallic properties analytically, by using a simplified version of the density of states. Figure 6 shows such a simplified ver-

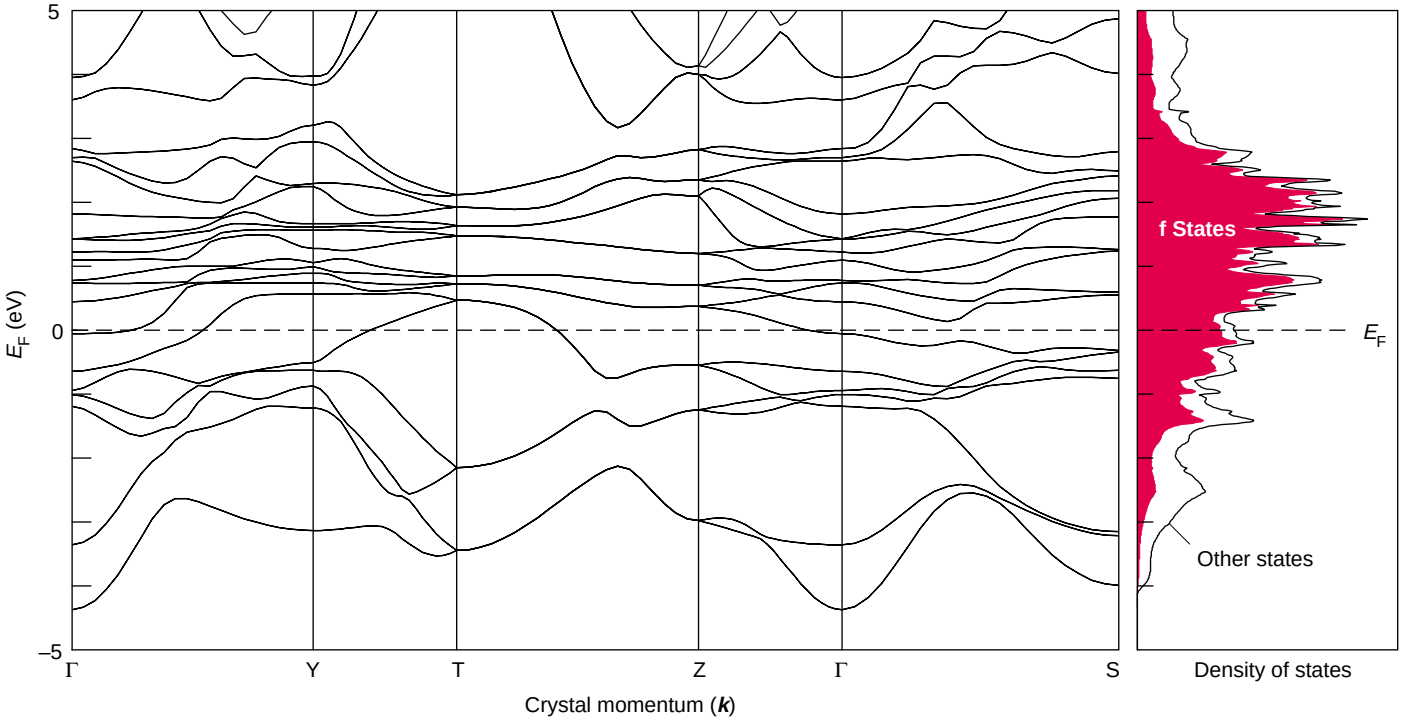

Figure 5. Calculated Energy Bands and Density of States of α-Uranium

DFT predictions for the energy bands *e*(*k*) are plotted along several different directions in the unit cell of the reciprocal lattice. The labels on the *k*-axis denote different high-symmetry points of the Brillouin zone: Γ = (000), Y = (110), and T = (111). The narrow bands close to the Fermi level (dashed line) are dominated by the 5f orbitals. The fact that some of the bands cross the Fermi level demonstrates that α-uranium is a metal. The shaded area of the density of states curve represents the contribution from the 5f orbitals.

sion called the Friedel model, which is applicable to the transition metals. The d band is represented by a constant density of states over a relatively narrow energy range, and the s and p bands are represented by a much-broader, combined band. The figure also indicates the atomic energy level from which the d or f band originated. The band states at energies lower than the atomic energy level are bonding, and those at higher energies are antibonding.

Three decades ago, Friedel (1969) used this simplified density of states to explain the parabolic behavior of the equilibrium volumes of the 5d transition metals. He suggested that the cohesive energy of those metals varies with increasing atomic number because of the filling of a d-electron conduction band. The occupied states for the lighter elements would be bonding whereas for the heavier elements the occupied states would be both bonding and antibonding. Assuming a constant density of states for the d band as shown in Figure 6, Friedel wrote down the following analytical expression to approximate the contribution of the d band to the cohesive energy as a function of N_d, the number of valence electrons of the element (Friedel 1969):

$$E_{coh}(N_d) = -\frac{1}{2} W_d N_d \left(1 - \frac{N_d}{10}\right) , \qquad (14)$$

where W_d is the width of the d band. Note that 10 is the maximum value of N_d because an atom's d shell can have 10 electrons (5 orbitals × 2 spin states) at the most. This expression for the cohesive energy demonstrates that the chemical bonding is maximized for a half-filled shell ($N_d = 5$) and that the cohesive energy varies as $(N_d)^2$, or parabolically, when plotted as a function of N_d (see Figure 7). It also shows correctly that the cohesive energy is zero for a filled or an empty band. Because there is an inverse relationship between bond length (lattice constant or atomic radius) and bond strength (Pettifor 1995), the parabolic trend in the observed equilibrium volumes of the transition metals (see Figure 1) follows directly from this result for the cohesive energy.

The Friedel model also explains the parabolic behavior of the volumes of the actinides, but the 5- to 10-eV width of the d band must be replaced with the 3- to 4-eV width of the f band (Skriver et al. 1978, Skriver et al. 1980, Brooks et al. 1984). The agreement between theory and experiments suggests that the chemical binding of the transition metals and the light actinides is predominantly similar to the binding of metals; that is, the 5f electrons of the

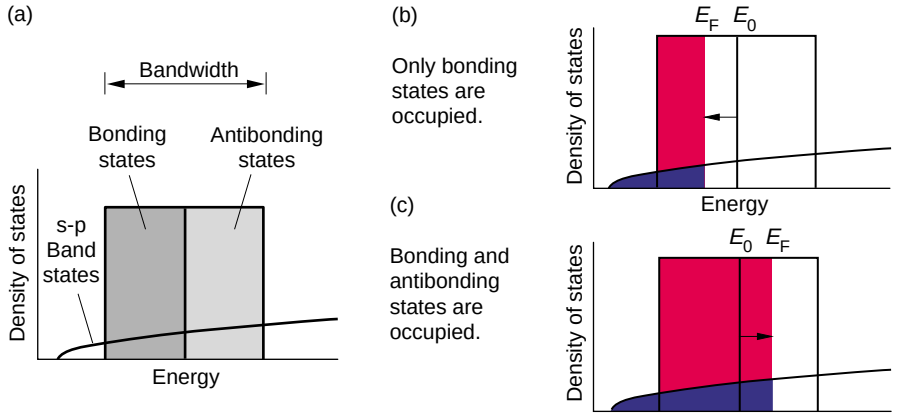

Figure 6. Density of States in the Friedel Model

(a) Shown here is a simplified form for the density of states called the Friedel model, which is applicable to the transition metals. The d band has a constant density of states over a relatively narrow energy range, and the s and p bands are represented by a broader, combined s-p band. E_0 is the atomic energy level from which the d band originated. The band states at energies lower than E_0 are bonding, and those at higher energies are antibonding. (b) For elements in the first half of the series, the Fermi level is below E_0, and all occupied states are bonding. (c) For elements in the second half of the series, the Fermi level is above E_0, and both bonding and antibonding states are occupied.

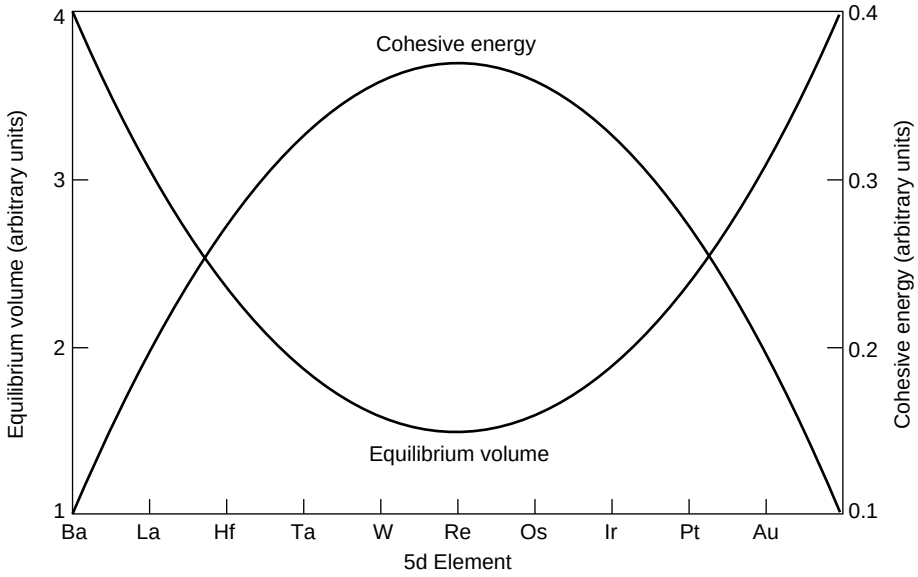

Figure 7. Friedel Model Predictions for the Cohesive Energies and Equilibrium Volumes of the 5d Transition Metals

The contribution of the d band to the cohesive energy is plotted as a function of N_d, the number of valence d electrons in each 5d transition metal according to Equation (14). The chemical bonding reaches a maximum for a half-filled d shell ($N_d = 5$), the cohesive energy from the d band varies parabolically, and its value is zero for a filled or an empty band. Because the equilibrium volume varies inversely to the cohesive energy, the parabolic trend in the observed equilibrium volumes of the transition metals (see Figure 1) follows directly from this result for the cohesive energy.

light actinides are conduction electrons participating in bonding.

The behavior of the light actinides deviates in one way from the parabolic behavior predicted by the Friedel model: The volume of plutonium is actually larger than that of neptunium even though the f band is not yet half filled (the f shell can have a maximum of 14 electrons—(7 orbitals × 2 spin states)—whereas plutonium in the solid state has only five 5f electrons). It was first thought that very strong spin-orbit interactions in the light actinides might split the single, narrow band in the Friedel-like density of states shown in Figure 6. In that case, the lower energy band would extend from thorium to americium, the cohesive energy would reach a maximum between uranium and neptunium, and plutonium would have a larger volume than neptunium (Skriver et al. 1978, Skriver et al. 1980, Brooks et al. 1984). Our subsequent, more-accurate calculations have shown that the spin-orbit interactions alone are insufficient for explaining the upturn in volume between neptunium and plutonium. Indeed, we had to use both the correct crystal structure of α-plutonium and the best available estimate of the exchange and correlation potential (obtained with the GGA) to reproduce that observation (see our results in Figure 4). This modification of the Friedel model, however, is very slight, and in no way alters the main conclusion that the 5f states in α-plutonium are delocalized in very much the same way as those in α-neptunium and α-uranium.

Actinide Structures

Having shown that the light actinides and the transition metals agree with the Friedel model of chemical bonding, we return to the question of whether this similarity in bonding is compatible with the very different structural properties of the actinides and transition metals. Recently, together with our collaborators, we have investigated the structural stability of the

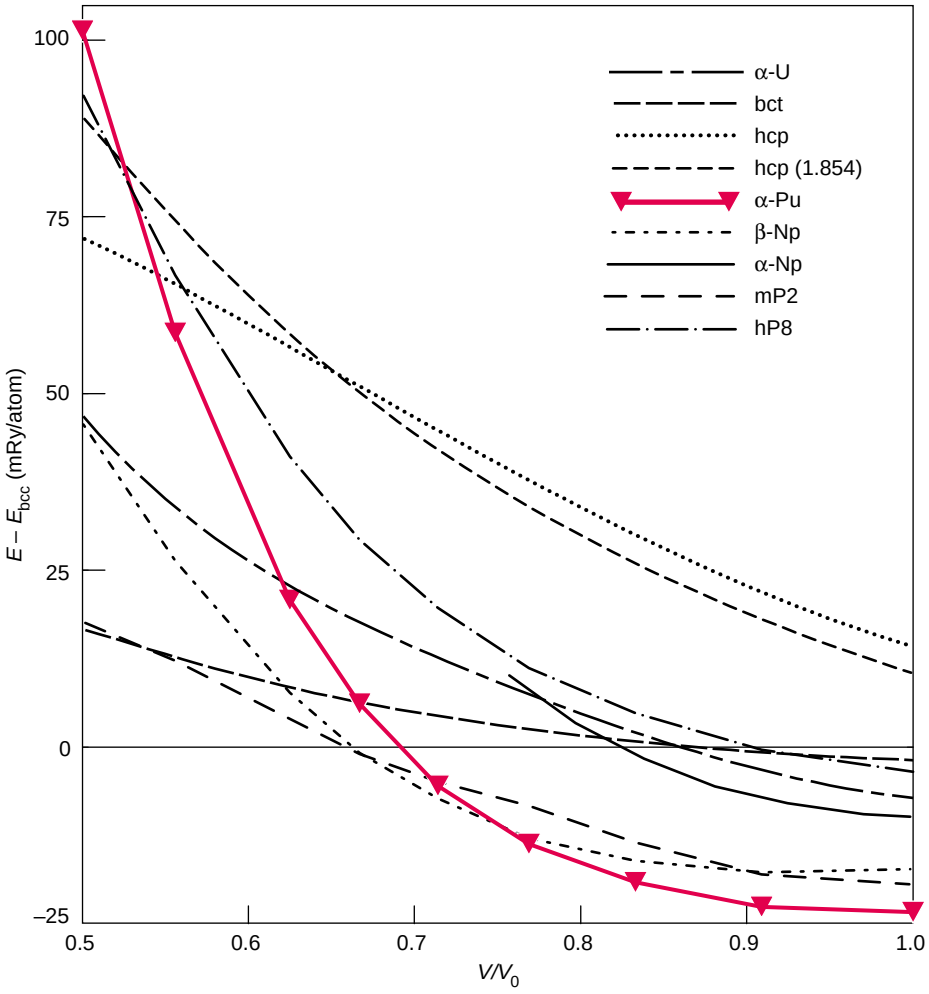

Figure 8. DFT Energies for Plutonium in Different Crystal Structures as a Function of Compressed Volume

Of all the plutonium structures used as input to the calculations, the α-plutonium structure yielded the lowest energy at the equilibrium volume. The delocalized bcc phase is the reference level and is set to zero. V_0, the equilibrium volume of α-plutonium, is 19.49 Å^3. Under a sufficiently high pressure, calculation predicts that most of the light actinides—uranium, neptunium, and plutonium—revert to a highly symmetric bcc structure.

actinides (Wills and Eriksson 1992, Söderlind et al. 1995, Söderlind 1998). Using our DFT methodology, we were able to calculate the total energy of the transition metals and the light actinides in various crystal structures to an accuracy of thousandths of an electron-volt, or approximately 0.1 to 0.5 millirydberg (mRy). With this theory, we successfully reproduced the stability of the low-symmetry structures of the light actinides. As an example, Figure 8 displays the calculated energies of different structures of the most complex actinide material, plutonium. Of all the investigated structures, the α-plutonium structure (which is monoclinic with 16 atoms per unit cell) is correctly calculated to have the lowest energy. We also predict that, under a sufficiently high pressure, most of the light actinides (uranium, neptunium, and plutonium) will revert to the highly symmetric bcc structure. Recent diamond-anvil-cell experiments confirm these predictions for neptunium.[4]

In 1970, Hunter Hill proposed that the unusual structures found in the light actinides resulted from covalent bonding between the highly angular, or "pointed," orbitals of the 5f electrons (Hill and Kmetko). We have used first principles calculations to investigate this argument in detail and found that Hill's proposed mechanism is not correct. If Hill were right, one would expect the charge density, which is dominated by 5f electron states, to pile up between the actinide atoms. The contour plots in Figure 9 display the calculated charge density of α-uranium and silicon. The α-uranium plots (a–c) are in the 010-plane for three different cases. The first case includes the effects of the 5f binding, and the second one excludes the 5f binding. The two plots are almost identical. Hence, the shape of the charge density does not appear to be affected by the pointed 5f orbitals. In fact, the third charge-density contour plot, which shows the results of overlapping the charge densities of isolated atoms and therefore carries no information about the chemical bonding of the crystal, looks very similar to the first two plots. We conclude that, for α-uranium and other light actinides, the geometry of the underlying lattice determines the shape of the charge density. By contrast, for the heavy actinides, the charge density of the 5f atomic orbitals determines the geometry of the lattice. Finally, Figure 9(d) shows the charge density of silicon in the diamond structure, in which case strong covalent bonds do indeed cause a visible buildup of charge between the silicon atoms. The bond in α-uranium, on the other hand, is very weakly covalent (the chemical bonding in all materials has some degree of covalency), and the binding is best described as metallic.

Recently, R. C. Albers of Los Alamos and coworkers made calculations for aluminum that seem to support Hill's conjecture. By using an enlarged

[4] J. Akella, Lawrence Livermore National Laboratory (private communication).

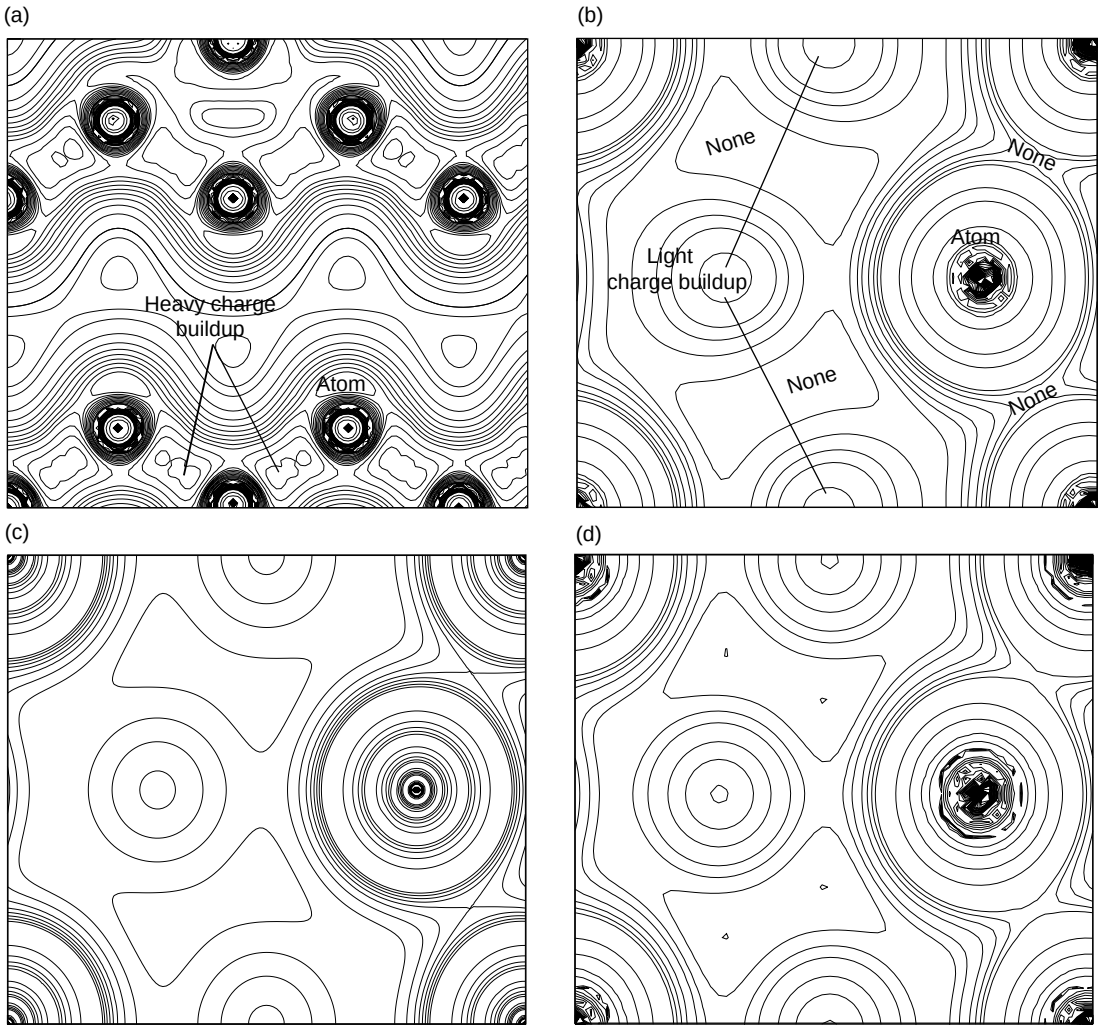

Figure 9. Calculated Charge Density of α-Uranium and Silicon in the 010-Plane

We compare three electron-density contour plots of α-uranium with a similar plot for silicon in the diamond structure. Shown in (a) is the plot for silicon. In the diamond structure, silicon provides an excellent example of covalent bonding, the signature of which is a buildup of charge along bonds. In contrast, the uranium contours (b–d) show a buildup of charge away from the bonds, in the interstices. This type of buildup is characteristic of metallic bonding. However, the underlying lattice often determines the appearance of an electron-density contour. We are, therefore, showing three kinds of calculations for uranium: In (b), we calculated the electron density with itinerant 5f electrons, in (c) with core (spherical) 5f electrons, and in (d) by overlapping atomic densities. Clearly, the presence or absence of asymmetric 5f orbitals has little effect on the shape of the charge density and on the character of the bonds in α-uranium.

volume as the input, these scientists found the ground-state structure of aluminum to be the highly symmetric diamond structure. They suggested that, at the expanded volume, the very small overlap between atomic orbitals reduces the effects of the valence electrons on the nearest neighbors, and the angular character of the orbitals stabilizes the diamond structure. We have checked this conjecture by calculating the total energy of aluminum first in the diamond structure and then in a series of lower symmetry orthorhombic structures. This crystal distortion actually leads to a structure resembling that of γ-plutonium. Plotted in Figure 10, our results show that the diamond structure is not the lowest energy structure of aluminum at expanded volumes. Instead, a low-symmetry actinide-like structure is the most stable.

A Mechanism for Stabilizing Low-Symmetry Structures. Our results for aluminum jibe with our understanding that the light actinides form in unique, low-symmetry open-packed structures because their f electrons occupy very narrow conduction bands (Wills and Eriksson 1992, Söderlind et al. 1995). The mechanism producing the low symmetry resembles a Peierls-Jahn-Teller distortion of the energy bands

and may be viewed as follows: Suppose an actinide metal is in a hypothetical bcc structure at ambient conditions and has an energy band shaped like the black curve in Figure 11. This band describes energy levels along a high-symmetry direction of the bcc crystal and therefore has a high degeneracy, say 2. In other words, there are two states for each energy level, and the energy band is really two bands of energy levels that lie on top of each other. (This type of degeneracy always occurs along high-symmetry directions of fcc and bcc structures). If the bcc structure were changed to a slightly distorted (say tetragonal or orthorhombic) bcc structure, the lowered symmetry would break the degeneracy. As shown in Figure 11, the original band would split into two nondegenerate bands: One would be slightly raised (the red curve) and the other slightly lowered in energy (the blue curve).

The hypothetical bands in Figure 11 are conduction bands; that is, they are intersected by the Fermi level E_F. Consequently, when the original band splits, some states are pushed above the Fermi level and others below that level. In fact, there is a range of wave vectors ***k***, in which the occupied states (those below the Fermi level) of the distorted structure are lower in energy than the occupied states of the symmetric structure. Thus, the energy contribution of those regions of ***k***-space is less in the distorted than in the undistorted structure. In other regions of ***k***-space, the contribution to the total energy is the same regardless of symmetry: Either both split bands are above E_F and therefore unoccupied (and not affecting the total energy), or they both are below E_F. In the latter case, the energy from the two split bands is equal to two times the average energy of those two bands, which is exactly the energy of the two degenerate bands of the high-symmetry structure. Thus, only regions of ***k***-space that straddle the Fermi level contribute to lowering the total energy of the low-symmetry structure. This energy-lowering mechanism is similar to the

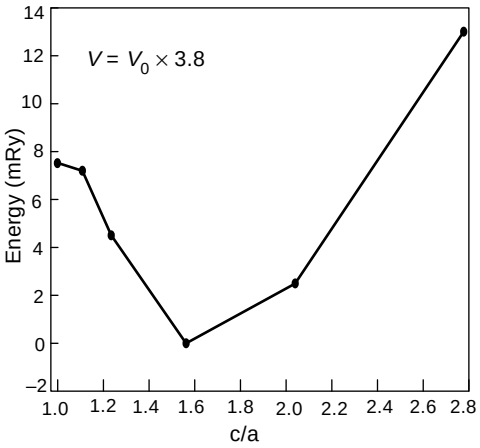

Figure 10. Calculated Total Energy of Aluminum as a Function of Orthorhombic Shear

Illustrated here is the energy of aluminum at 3.8 times its equilibrium volume. Starting from the diamond structure, we allowed the atoms to have orthorhombic and internal positional freedom. The resulting relaxed structure is very similar to that of γ-plutonium. This similarity illustrates the point that actinide structures are favored at narrow bandwidths even in non-f-bonded metals.

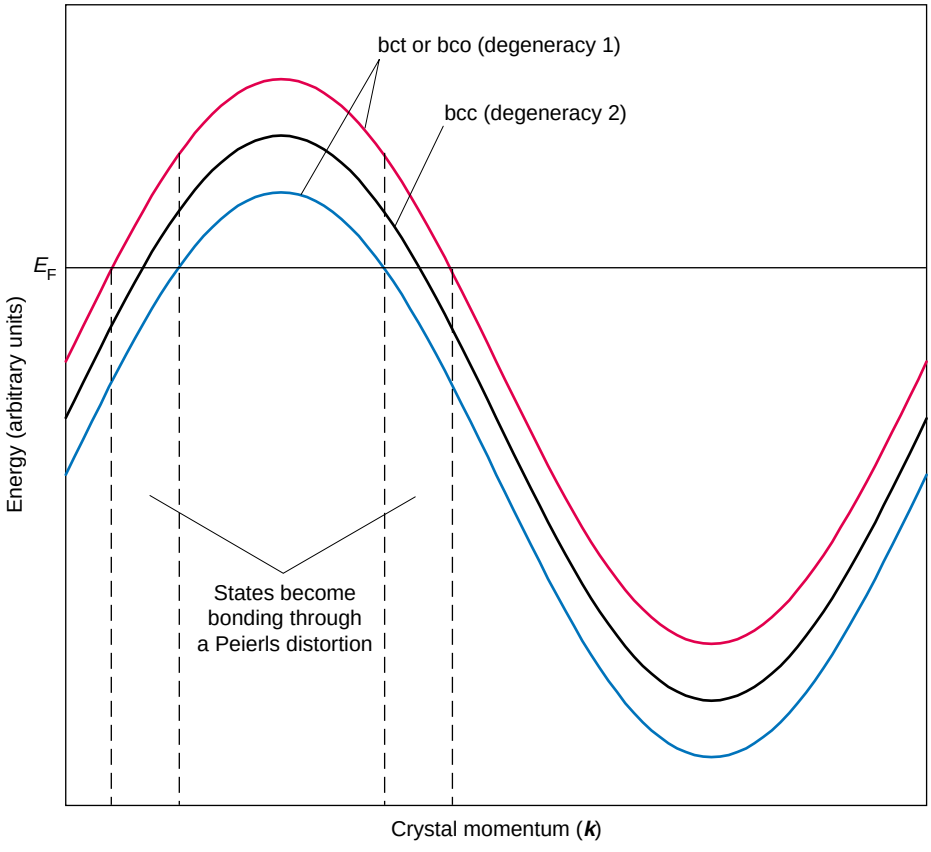

Figure 11. Lowering the Energy through a Peierls Distortion

The black curve is a hypothetical narrow energy band *e*(*k*) along a direction of high symmetry in a highly symmetric (bcc) crystal. The band passes through the Fermi energy and has a degeneracy of 2. If the crystal is distorted from a bcc to a bct or boc structure, the band splits into two nondegenerate bands (red and blue). In the two regions of *k*-space marked by dashed lines, occupied states that were near the Fermi energy in the bcc structure are lowered in energy and therefore lower the total energy. Other unoccupied states are lowered and become occupied. Therefore, the one-electron contribution to the total energy in those regions is lowered by a distortion to a lower-symmetry structure. In other regions of *k*-space, the contribution to the total energy is the same regardless of symmetry.

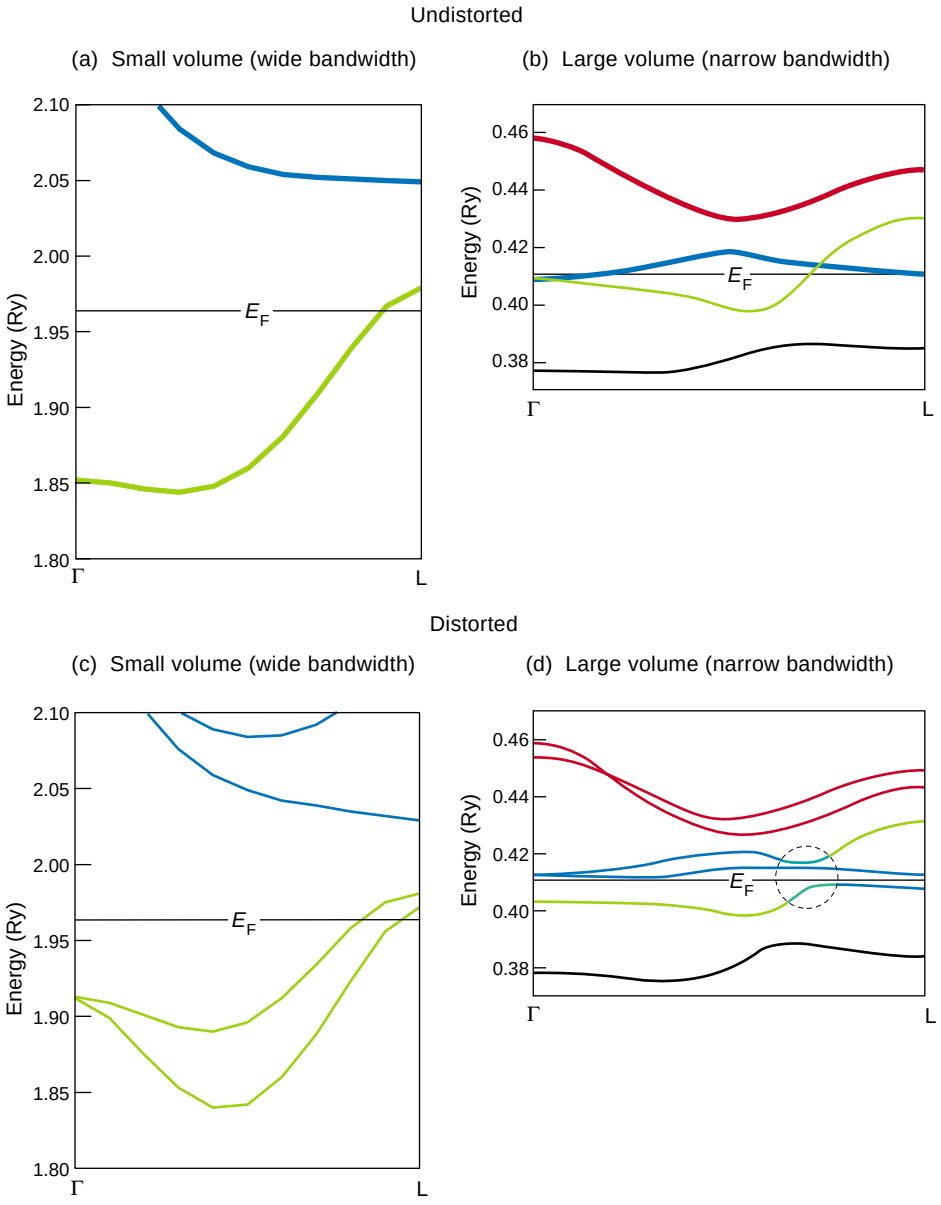

Figure 12. Calculated Energy Bands for Neptunium (bcc vs bct Structures)
We display the energy band structure in neptunium for two input volumes and two crystal structures. In the graphs to the right, the input volume is close to the equilibrium value for neptunium, the bands are narrow, and a distortion from bcc to bct pushes some states from just above to just below the Fermi level (see region within dashed circle), thereby lowering the one-electron contribution to the energy. In the graphs to the left, the input volume is compressed, the bands are therefore broader, and the splitting of these bands by a crystal distortion has no effect on the one-electron energy contribution. Thus, the narrow bands in neptunium explain its low-symmetry ground-state structure.

Peierls distortion and Jahn-Teller effect.

If the energy bands in Figure 11 were narrower (that is, if the curves were flatter), more states (or a larger region of the horizontal axis) would contribute to lowering the total energy of the distorted structure. This effect is seen in Figure 12, in which the calculated energy bands are shown for bcc neptunium and for a slightly tetragonally distorted (bct) structure of neptunium, each at two different volumes. For both the large and the small input volumes, the crystal distortion lifts degeneracies, lowering the energy of one band and raising the energy of the other, but at expanded volumes, the bands are flatter (narrower), and more electron states contribute to lowering the energy of the distorted structure.

The tendency toward expanded volumes and low-symmetry structures is balanced by other contributions to the total energy (such as electrostatic interactions and overlap repulsion) that favor broader bands and close-packed structures. Thus, the energy-lowering mechanism described here will lead to low symmetry only in systems with bands that are both narrow and intersected by the Fermi level (Wills and Eriksson 1992, Söderlind et al. 1995). The light actinides fulfill these two criteria.

The importance of the narrow bandwidth in producing low-symmetry structures is apparently independent of whether the electrons in the band originated from s, p, d, or f valence states. Figure 13 shows the calculated total energies of p-, d-, and f-bonded elements (aluminum, iron and niobium, and uranium, respectively) as a function of bandwidth for different crystal structures. The total energies for the fcc, bct, and α-uranium structures are plotted relative to the energy of the bcc structure. In these calculations, varying the input volume produces changes in bandwidth, and the total energy and the bandwidths are outputs. For all these elements, very low symmetry actinide-like structures are the most stable (lowest energy) configurations when the bands are narrow, and higher-symmetry structures are stable for broad bands. Note that in using the structure of α-uranium as an example of low symmetry, we do not imply that an α-structure is the most stable kind for all the other actinides.

DFT Calculations of the Charge-Density Wave. An extremely intricate connection between electronic and structural properties is the charge-density wave. Because of specific interactions between the electrons and the lattice, the charge density abandons the

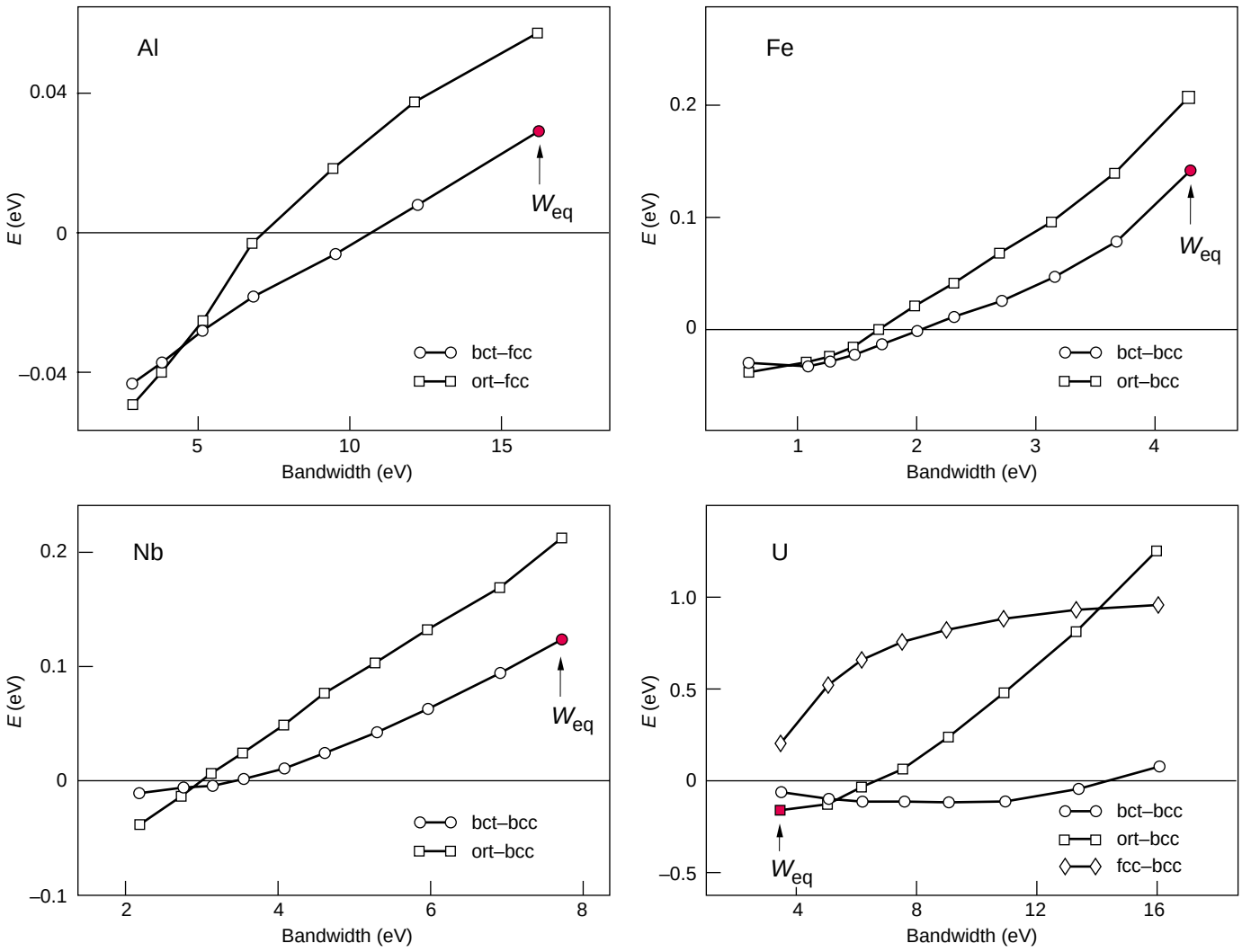

Figure 13. Calculated Total Energy of Different Crystal Structures as a Function of Calculated Bandwidth
In (a) through (d), we plot the DFT results for the total energies of aluminum (p-bonded), iron (d-bonded), niobium (d-bonded), and uranium (f-bonded) as a function of bandwidth for several different structures. We vary the bandwidth by varying the input volume. For all these elements, very low symmetry structures, similar to those of the actinides, are most stable configurations when the bands are narrow. High-symmetry structures, on the other hand, are stable for broad bands. The reference level (fcc for aluminum and bcc for the other metals) is set to zero. W_{eq} is the calculated bandwidth at the experimental equilibrium volume. Thus, if we use the observed equilibrium volumes, we predict that the transition metals will have broad bands and symmetric structures, whereas the light actinides will have narrow bands and low symmetry structures. (This figure was reproduced courtesy of *Nature*.)

perfect periodicity associated with the Bravais lattice and becomes a modulated function in space, with an oscillation period ranging, theoretically, over thousands of atoms. As a result, the atoms of the lattice move out of the position normally dictated by the Bravais lattice vectors and, instead, follow the periodicity of the charge-density wave.

The charge-density wave was originally proposed to occur in s-band metals such as sodium (Overhauser 1971), but as is often the case with interesting new physics, the only element that actually exhibits the new phenomenon is an actinide. After many decades of thorough experimental work, it was established that uranium metal goes through a sequence of distinct low-temperature phases and that those phases are different charge-density waves called α_1, α_2, and α_3 (Smith et al. 1980, Lander et al. 1994). The first transition takes place at 43 kelvins (α_1), and the last one stabilizes at 23 kelvins (α_3). After the completion of the last charge-density-wave transition, the approximate volume of the unit cell is a staggering 6000 cubic angstroms per primitive cell.

Smith et al. (1980) and Lander et al. (1994) have identified the charge-

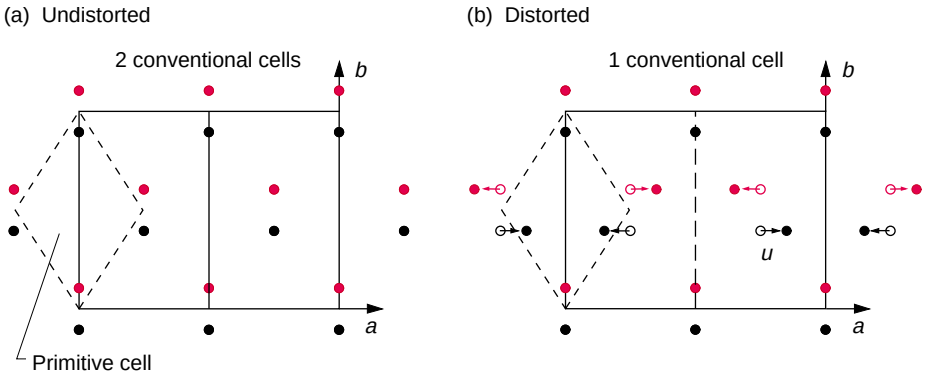

Figure 14. Structural Distortion Associated with the α_1 Charge-Density Wave of Uranium

Uranium metal goes through three distinct low-temperature phases, which are charge-density waves called α_1, α_2, and α_3. We calculated the transition to the α_1 state. The figure shows the crystal structure before and after the transition to the α_1 charge-density wave (the structures are projected onto the a-b plane). The conventional unit cell doubles as atoms are displaced by an amount *u* along the *a*-direction. In each structure, the black (red) circles mark atoms situated in the c = 0 (c = 1/2) layer, respectively.

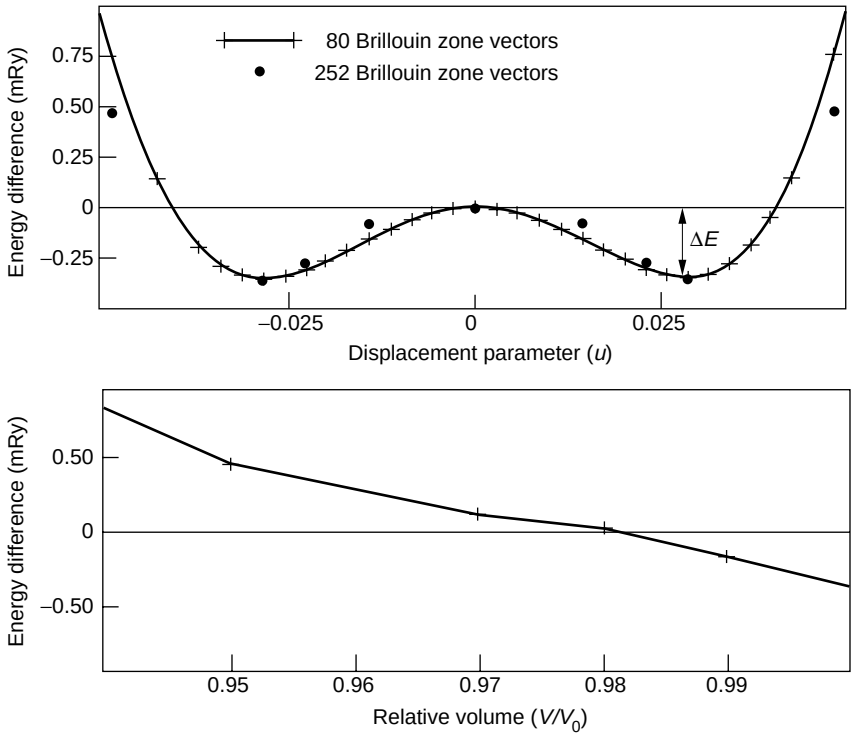

Figure 15. Calculated Energy Dependence of the α-Uranium Charge-Density-Wave Distortion

In both plots, the horizontal line represents the energy of α-uranium, and the energy of the α_1-phase (charge-density wave) is plotted relative to it. (a) The calculated energy of the α_1-phase at ambient conditions reaches a minimum for a displacement parameter (*u*) value of 0.028. This value agrees well with the experimental one of 0.027. (b) The calculated energy of the α_1-phase increases as the volume is compressed, and at a compression of $V/V_0 = 0.98$, the α_1-energy becomes higher. In other words, the α_1-phase should disappear at this compression. This prediction agrees well with the observed transition at a compression of $V/V_0 = 0.99$.

density-wave state in uranium through structural changes. Transmission electron microscopy shows well-characterized twin/tweed patterns in the charge-density-wave state and reveals a most-pronounced shape memory effect. Neutron scattering experiments indicate that significant phonon softening occurs in the charge-density-wave state at 43 kelvins. Knowing this fact may be helpful in understanding this martensitic transition.

From a materials science point of view, the charge-density-wave state in uranium manifests itself by a small distortion, which has a drastic effect on several physical properties: lattice parameter, resistivity, elastic response, and thermal expansion (Smith et al. 1980, Lander et al. 1994). The physical mechanisms driving the different charge-density waves in uranium are similar, and for that reason, as well as for practical reasons, we focused on calculating the transition to the α_1-state. In this transition, the conventional unit cell doubles as atoms are displaced by an amount *u* along the *a*-direction, according to the pattern shown in Figure 14. In Figure 15, the calculated total energy of uranium in the doubled unit cell is shown as a function of the displacement parameter *u*, which serves as the order parameter for the transition (Fast et al. 1998). Note that the total energy reaches a minimum at $u = 0.028$, which agrees almost perfectly with the experimental value of 0.027. Note also that, because the energy involved in this transition is minute, tremendous demands are placed on the theoretical method.

We have performed similar calculations for compressed volumes. At a compression of $V/V_0 = 0.98$, the total energy of the α_1 state becomes higher than the energy of the α-uranium structure, that is, the calculation predicts that the charge-density wave disappears. The calculated result agrees well with the observed transition at a compression of $V/V_0 = 0.99$. Here again, compressed volumes (and the resulting broadened bandwidths) destroy the more-complex less-symmetric structure in favor of

the more-symmetric one.

The specific mechanism driving the transition to the charge-density-wave state involves a feature of the energy bands and the Fermi surface called "nesting" (that is, many sheets of the Fermi surface are connected by vectors of similar length and direction). It is again a Peierls-like mechanism (Fast et al. 1998), but a much smaller part of the Brillouin zone is involved relative, for example, to the region that stabilizes plutonium in the low-symmetry α-plutonium structure.

In closing this section, we note that the fine details of the structural properties of the light actinides shown here reflect a very accurate treatment of the density, potential, and wave functions, in addition to all the relativistic effects. That accuracy was born from developments in theory and software over many years.[5]

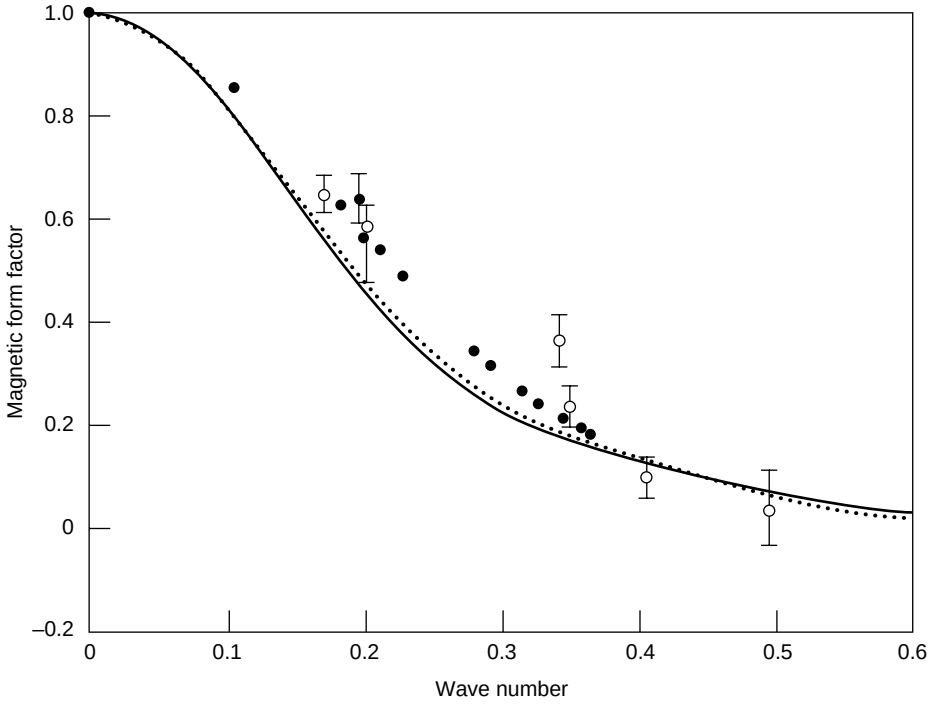

Figure 16. Calculated Field-Induced Form Factor of α-Uranium
We compare our DFT results for the field-induced magnetic form factor of α-uranium (full line) with experimental values (dotted line). The good agreement in both magnitude and shape of the spin density suggests that the DFT provides an accurate description of electronic structure in uranium.

Calculated Magnetic Susceptibilities of Uranium and Plutonium

Experiment has shown that all the light actinides are paramagnetic: Even at the very lowest temperatures, they do not spontaneously order in a magnetic configuration (they never become ferromagnets). Only when an external magnetic field is applied, does a small (positive) magnetic moment develop. This finding is consistent with the fact that the f electrons in the light actinides occupy band states rather than localized states.

To test the quality of the band picture further, we used the calculated set of bands to compute the field-induced magnetic moments of uranium and plutonium and compared our results with measured data for the magnetic susceptibilities and magnetic form factors (Hjelm et al. 1994). This is a sensitive test of our calculations. Good agreement means that our band calculation is accurate and the whole concept of itinerant states in the light actinides is appropriate. In these calculations, we include the so-called "Zeeman term," $\boldsymbol{B}(2\boldsymbol{S} + \boldsymbol{L})$, where $\boldsymbol{B}$ is the magnetic field in the Hamiltonian.

In an applied field of 7 tesla, the calculated field-induced moment in uranium is 4.7 millibohr magnetons ($m\mu_B$), and the experimentally measured value is 4.9 $m\mu_B$. There are no measurements of induced moments in α-plutonium, so we infer them from measured magnetic susceptibilities. In an applied field of 10 tesla, the calculated field-induced moment of α-plutonium is 8.4 $m\mu_B$, whereas the induced moment inferred from measured susceptibilities is 9.8 $m\mu_B$. We have also calculated the field-induced magnetic form factor for α-uranium. The magnetic form factor is simply the Fourier transform of the field-induced magnetization density, which we can calculate from spin DFT. Figure 16 compares the experimental and theoretical magnetic form factors and shows good agreement between them. Hence, DFT calculations reproduce the magnitude of the field-induced moment, as well as intricate details concerning the shape of the spin density for both α-uranium and α-plutonium, confirming that a band picture is appropriate for these two elements.

A Mott Transition in the Actinide Series

Because the question of electron localization and delocalization is central to actinide physics, we will note here that the variation of the energy levels with $\boldsymbol{k}$, also called the energy dispersion, is a good measure of how localized the electrons are. Little dispersion, or a narrow energy band,

[5] J. M. Wills, software package FP-LMTO (Los Alamos National Laboratory, Los Alamos, New Mexico, unpublished).

means that each conduction electron is close to being localized on an atomic site and, hence, spends a long time around this site before it jumps to the next site. The longer an electron is localized to a given nucleus, the more atomic-like its behavior, and the narrower the band. When the bandwidth becomes sufficiently narrow, the electrons localize and stop being itinerant. In practice, one expects localization to occur when the energy associated with the electron-electron interaction (correlation) is about the same size as the energy bandwidth.

To understand the effects of electron correlations, one traditionally turns to model Hamiltonians, such as the expression in Equation (1). That Hamiltonian can be augmented to incorporate electron-electron correlations. One such possibility would be

$$H = e\sum_{i\mu}\hat{n}_{i\mu} + h\sum_{i\mu}\sum_{j\neq i,\nu}\hat{c}^{\dagger}_{j\nu}\hat{c}_{i\mu} + U\sum_{i\mu\nu}\hat{n}_{i\mu}\hat{n}_{i\nu} \quad , \qquad (15)$$

where we now consider a degenerate atomic level with energy e and orbitals μ on lattice sites i. In contrast to the Hamiltonian in Equation (1), this Hamiltonian has two competing terms: the hopping term (proportional to h), which tends to lower the energy if electrons are shared between atoms, and the on-site Coulomb term (proportional to U), which raises the energy if electrons are shared between atoms. When the ratio h/U is small, the electronic states of such a Hamiltonian are substantially localized and may, in a good approximation, be considered to belong to one atom or another. This is the low-density limit of an elemental solid. When h/U is large, the electronic states of such a Hamiltonian are substantially itinerant, and the band picture, which was described in the earlier sections, is a good approximation. In the latter case, which is the high-density limit of a solid, exchange and correlation are included in an average way, as in the LDA. At some point in the transition from low to high density, it becomes energetically favorable for electrons to hop between atoms, and the system undergoes a Mott transition.

The density at which it becomes energetically favorable to delocalize depends on the atomic number and the orbital character of the atomic valence states. States with a small angular-momentum barrier (s and p states) delocalize easily, whereas states with a larger angular-momentum barrier (d and particularly f states) retain their atomic character to higher densities. With the exception of the lanthanides past cerium and the actinides past plutonium, elements at zero pressure and low temperature have a delocalized, or itinerant, electronic character, and are well described by band theory.

Now, let us return to Figure 1 for a moment. As mentioned earlier, the volume and structure of americium (and of the elements following it) are drastically different from those of the light actinides. This finding was observed many years ago. Skriver et al. (1978), Skriver et al. (1980), and Brooks et al. (1984) explained it by assuming a Mott localization of the 5f shell. Therefore, the 5f states are localized and chemically inert in americium, just as they are in the rare-earth elements. As a result, the chemical bonding provided by the 5f electrons is lost, and the equilibrium volume is increased. In addition, the narrow 5f band pinned at E_F in the light actinides is absent in americium, and the mechanism for driving open and/or low-symmetry structures is lost. Thus, americium has a well-behaved double hexagonal close-packed (dhcp) structure, which is found frequently among the lanthanides.

We may explain the localization of the 5f electrons in americium by comparing the way in which the energy is lowered through band formation (itinerant electrons) and through multiplet formation (localized electrons). The idea is that the 5f electrons in americium form an atomic multiplet in a "Russell-Saunders coupling." This strongly coupled formation lowers the repulsive energy generated by the electron-electron interactions. At the same time, the strong coupling in the multiplet also lowers the total energy by an amount $\Delta_{coupling}$. This lowering in energy should be compared with that stemming from band formation, E_{band}. It has been demonstrated that, for the light actinides, the energy is mainly lowered through band formation whereas for americium and the actinides after americium, it is lowered through multiplet formation (Skriver et al. 1978, Skriver et al. 1980, Brooks et al. 1984). The ground-state, localized 5f atomic multiplet of americium corresponds to a total angular momentum of zero, $J = 0$, which explains why no magnetic ordering occurs in this material. It was even observed (Smith and Haire 1978) that americium becomes superconducting at low temperatures. This observation agrees with predictions (Johansson and Rosengren 1975).

The δ-Phase of Plutonium

Thus far, we have outlined what may be viewed as a rather successful theoretical description and understanding of the ground-state physics of the light actinides. In the final section of this article, we outline an important problem of actinide physics and chemistry, which has escaped most researchers' attention.

From Figure 1, we see that the actinide series naturally divides into two parts: an early part, in which the 5f states are delocalized and chemically active, and a later part, in which the 5f states are localized, atomic-like, and chemically inert, as are most rare-earth elements, However, one allotrope of plutonium, the δ-phase, does not categorize well into either of the groups (all plutonium allotropes other than α-plutonium may be hard to categorize in a simple way, but we will not address that issue here). One should note here that the δ-phase is observed at elevated temperatures, but it may be stabilized at low

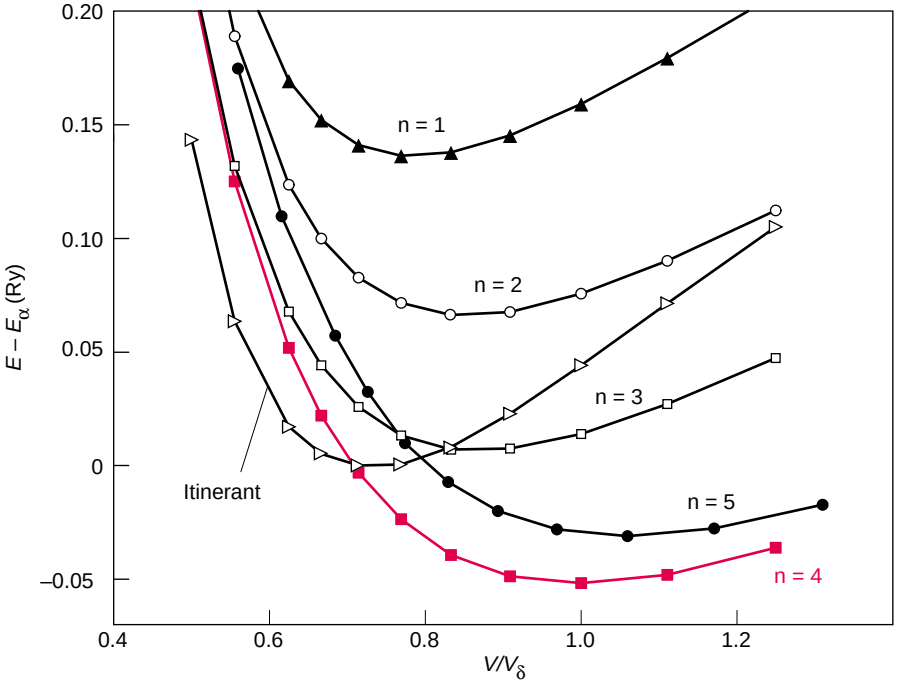

Figure 17. Energy of fcc Plutonium for Different Numbers of Localized 5f Electrons

Each curve shows our results for the total energy of δ-plutonium relative to that of α-plutonium as a function of V/V_δ. The curves are labeled by *n*, the number of localized 5f electrons assumed for those calculations. The curve that predicts the lowest energy at the correct δ-plutonium volume, $V/V_\delta = 1$, is the configuration with four of the 5f electrons localized and only one itinerant. Moreover, the energy of this state relative to the α-phase is about right.

temperatures when we add a few atomic percent of aluminum, gallium, or cerium.

As seen in Figure 1, the volume of δ-plutonium is between that of α-plutonium and americium. If the 5f electrons of δ-plutonium were localized, the equilibrium volume would be close to that of americium, and if the 5f electrons were delocalized, the equilibrium volume would be close to that of α-plutonium. Instead, δ-plutonium has an intermediate volume, indicating that the 5f electrons are in some unknown intermediate state. Thus, the traditional view that electrons localize between plutonium and americium needs to be modified and allow for an in-between phase represented by δ-plutonium.

In addition to its unusual equilibrium volume, δ-plutonium has an exotic negative thermal expansion—upon heating, the volume decreases. According to the conclusions drawn in the previous section, if the 5f states were delocalized in δ-plutonium, the structure of this allotrope would be distorted. Therefore, the observed fcc structure of δ-plutonium suggests that the 5f states, like those in α-plutonium, are not delocalized. Moreover, if the 5f states were localized, as they are in americium, one would expect (from atomic theory) that they would couple to give a magnetic moment for each plutonium atom, and as a consequence, one would observe magnetic ordering in the crystal at low temperatures. Although experiments on this allotrope are quite sparse, the question of whether a temperature-dependent magnetic susceptibility has been observed in plutonium above the α-phase is currently controversial. If such a behavior could be confirmed, a conclusion about the existence of local moments (indicating the 5f localization) could be confirmed.

Our most-recent efforts have addressed this problem (Eriksson et al. 1999). We have modified the energy expression in Equation (7) to incorporate states that are a mixture of localized and delocalized states, a mixed-level approximation. With this expression, we calculated the total energy as a function not only of volume and structure but also of the fraction of the electron density that corresponds to localized electrons. By using the Russell-Saunders coupling, we calculated the total energy of any localized part of the 5f electron sea.

We achieve the mixed-level approximation by imposing a constraint on certain electrons so that they become localized. The constraint is that these electrons should not hop from site to site and should not mix (hybridize) with any other electron states. One can perform a constrained calculation using the method outlined in our discussion of Equation (4). However, because of the constraint, the total energy is now larger than that obtained from the unconstrained LDA calculation, $E = E_{\mathrm{LDA}} + \Delta_{\mathrm{constraint}}$. One may now associate the localized f configuration with an uncoupled (that is, in terms of the Russell-Saunders coupling) atomic configuration. This configuration is sometimes called the grand barycenter of an atomic configuration.

From atomic theory, one can calculate the energy difference between this configuration and the lowest atomic multiplet. Because such a description becomes quite lengthy, we simply refer to this energy as $\Delta_{\mathrm{coupling}}$. A true estimate of the total energy of a 5f localized configuration of an actinide material should therefore be $E = E_{\mathrm{LDA}} + \Delta_{\mathrm{constraint}} - \Delta_{\mathrm{coupling}}$. In this expression, all terms can be calculated. If they are applied to americium metal, the localized f^6 configuration has the lowest total energy, in agreement with experiment. This approach is not phenomenological; it simply combines knowledge of DFT with knowledge of atomic theory (Russell-Saunders coupling). Some atomic-theory parameters are taken from experiments, but nothing prevents us from calculating these

parameters from, for example, configuration-interaction theories. A partitioning of the 5f manifold into localized and delocalized parts is physically reasonable, and one can investigate if the total energy is lowered by this procedure. In Figure 17, we show such a calculation for δ-plutonium, and we note that most of the ground-state properties (equilibrium volume and energy separation to the α-phase) of the δ-plutonium are reproduced with 4 localized electrons. The total energy is also lowest for this configuration. The good agreement between theory and experiment referred to here suggests that δ-plutonium is in a unique electronic configuration that has not been discussed before: The 5f manifold is partly delocalized and partly localized (Eriksson et al. 1999).

Summary and Outlook

We have outlined some of the more interesting aspects of the electronic structure of the actinides and especially how that structure relates to chemical bonding and structural properties. We argue that the presence of a narrow 5f band that is intersected by the Fermi level is the key ingredient for explaining the unusual structural aspects of the light actinides. From the research conducted in this past decade, a picture emerges of the physics of the unique actinide structures. From it, we can argue that most actinides should transform into high-symmetry structures (namely, bcc for uranium, neptunium, and plutonium) when they are compressed (Wills and Eriksson 1992, Söderlind et al. 1995). This prediction was recently verified for neptunium. A more extended discussion of these issues can be found in a recent overview article by Söderlind (1998).

The work on the low-temperature phases of the light actinides shows that the theoretical formalism of DFT, in the LDA or GGA, reproduces many of the ground-state properties, such as lattice constants, formation (cohesive) energy, structural properties, susceptibility, and elastic properties. It is our view that this method can then form a basis for the theoretical modeling of other more-practical aspects of materials, such as alloy formation, segregation profiles, stacking fault energies, and energies of grain boundaries.

In addition, we have presented evidence that the electronic configuration of δ-plutonium is unique in the periodic table. Hence, it is not only the structural properties of plutonium (for instance the low-symmetry structure of the α-phase) that are unique, but also the electronic ones. Before theory can make much more progress in explaining the complex phase diagram of plutonium, there is a great need for accurate experimental work to be performed on high-purity single crystals. (Comparison with the first photoemission data on pollycrystalline α- and δ-samples are encouraging but leave many unaswered questions, as discussed on page 152) A successful understanding of the plutonium phase diagram and especially δ-plutonium may help in answering questions about the stability of this allotrope. When considering stockpile stewardship, it is important to know if the impurity-stabilized δ-plutonium is a ground-state or a metastable phase. If it is a metastable phase, knowing its decay rate is very important. There are compelling reasons to expect that impurity-stabilized δ-plutonium has the same structure as temperature-stabilized δ-plutonium. There is also evidence that the same 5f bonding prevails in stoichiometric plutonium compounds as in δ-plutonium.

We have applied our theory to the plutonium-gallium compounds Pu_3Ga and PuGa and find good agreement between experimental and calculated volumes and energies—again with a partitioning of the 5f manifold into four localized states. In this paper, we have outlined a model for understanding the electronic properties of δ-plutonium. Although the proposed theory seems to work well, we need to see other, parallel attempts aimed at describing the correlated electronic properties of this allotrope of plutonium. As already indicated, this effort could involve theories based on the GW approximation or dynamical mean-field theory.

In future work, it will become important to have theoretical models for calculating the free energy of the actinide elements as a function of temperature. The theory presented here only applies to zero temperature. To include temperature effects, however, is a formidable task, and we must create some simplifications. A possibility is to integrate the existing expertise in molecular dynamics simulations with the expertise in electronic-structure and total-energy calculations. Alternatively, accurate calculations of the phonon spectrum of different allotropes may enable reliable calculations of the free energy as a function of temperature. With either of these approaches, one could then gain understanding about the structural and electronic properties of the different allotropes in the pressure-temperature phase diagram of the actinide elements. Also important in future work will be the application of the present DFT formalism to much larger systems in order to study the effects of impurities and segregation profiles for impurities, grain boundaries and their effect on materials properties, and finally, structural disorder. This last application is most important to investigate because there is a possibility that, without recourse to a more complex correlation than presently exists in DFT functionals, local deviations from a global structure might induce at least partial localization in plutonium.

Some of the results presented here show a recent trend in solid-state physics: Total-energy calculations are approaching an accuracy that enables a reliable and robust reproduction of experimental data, providing new insight into mechanisms pertinent to a given physical or chemical question. In addition, the calculations sometimes have become predictive, as they have for the high-symmetry structures of uranium, neptunium, and plutonium under compression. One can envisage that, in the near future, first principles calcu-

lations will be used in testing certain chemical and physical concepts about the actinides before a more cumbersome and expensive experiment is made. As for the electronic configuration of δ-plutonium, it has been revealed as truly novel in our calculations. The time has now come for experimental work on this interesting material to take a step forward and confirm or refute present theories of this material. ■

Acknowledgments

Most of this work has been collaborative. Our thanks for the excitement we have enjoyed over the physics of the actinides go to A. Balatski, D. Becker, A. M. Boring, L. Fast, A. Hjelm, B. Johansson, L. Nordström, H. Roeder, G. Straub, P. Söderlind, and J. Trygg. Nikki Cooper's critical reading and many useful comments are gratefully acknowledged.

Further Reading

Brooks, M. S. S., H. L. Skriver, and B. Johansson. 1984. In *Handbook on the Physics and Chemistry of the Actinides*. Edited by A. J. Freeman and G. H. Lander. Amsterdam: North Holland.

Dreitzler, R. M., and E. K. U. Gross. 1990. *Density Functional Theory*. Berlin: Springer.

Eriksson, O. D., D. Becker, and A. S. Balatski. 1999. *J. Alloys and Compounds* **287**: 1.

Fast, L., O. Eriksson, L. Nordstrom, B. Johansson, and J. M. Wills. 1998. *Phys. Rev. Lett.* **81**: 2978.

Friedel, J. 1969. *The Physics of Metals*. J. M. Ziman, ed. New York: Cambridge Univ. Press.

Georges, G., G. Kotliar, W. Krauth, and M. J. Rosenberg. 1996. *Rev. Mod. Phys*. **68**: 13.

Hedin, L. 1965. *Phys. Rev. A* **139**: 796.

Hill, H. H., and E. A. Kmetko. 1970. W. N. Miner, ed. *Nucl. Met.* **17**: 223.

Hjelm, A., J. Trygg, O. Eriksson, and B. Johansson. 1994. *Phys. Rev. B* **50**: 4332.

Hohenberg, P., and W. Kohn. 1964. *Phys Rev*. **136**: 864.

Johansson, B. 1974. *Phil. Mag*. **30**: 469.

Johansson, B., and A. Rosengren. 1975. *Phys. Rev. B* **11**: 2836.

Kmetko, E. A., and J. T. Waber. 1965. "Plutonium." In *Proc. 3rd Int. Conf*. London: Chapman and Hall Ltd.

Koelling, D. D., A. J. Freeman, and G. Arbman. 1970. W. N. Miner, ed. *Nucl. Met.* **17**: 194.

Kohn, W., and L. J. Sham. 1965. *Phys. Rev*. **140**A: 1133.

Lander, G. H., E. S. Fisher, and S. D. Bader. 1994. *Adv. Phys*. **43**: 1

Overhauser, A. W. 1971. *Phys. Rev*. B **3**: 3173.

Pettifor, D. 1995. *Bonding and Structure of Molecules and Solids*. Oxford: Oxford Science Publications.

Sandalov, I., O. Hjortstam, B. Johnasson, and O. Eriksson. 1995. *Phys. Rev*. B **51**: 13987.

Seaborg, G. T. 1945. *Chem. Eng. News* **23**: 2190.

Skriver, H. L., O. K. Andersen, and B. Johansson. 1978. *Phys. Rev. Lett*. **41**: 42.

———. 1980. *Phys. Rev. Lett.* **44**: 1230.

Smith. J. L., and R. J. Haire. 1978. *Science* **200**: 535.

Smith, H. G., N. Wakabayashi, W. P. Crummett, R. M. Nicklow, G. H. Lander, and E. S. Fischer. 1980. *Phys. Rev. Lett*. **44**: 1612.

Söderlind, P. 1998. *Advances in Physics* **47**: 959.

Söderlind, P., O. Eriksson, B. Johansson, J. M. Wills, and A. M. Boring. 1995. *Nature* **374**: 524.

Steiner, M. M., R. C. Albers, and L. J. Sham. 1992. *Phys. Rev. B* **45**: 3272.

Wills, J. M., and O. Eriksson. 1992. *Phys. Rev. B* **45**: 13,879.

John Wills graduated from the University of Hawaii in 1979 with a Bachelor's degree in physics and received a Ph.D. in physics from Stanford University in 1983. John worked as a postdoctoral researcher at West Virginia University from 1983 to 1986, when he became staff member in the theoretical Division at Los Alamos, where he is currently employed. He is the author of a full-potential electronic-structure method, the first method to be used successfully on cerium and the light actinides. A significant fraction of his research has been on the theory of the magnetic and structural properties of the actinides, which he has studied for the past fifteen years.

Olle Eriksson received his Ph.D. in condensed matter physics at the University of Uppsala in Sweden. Between 1989 and 1997, he was a postdoc, consultant, and a long-term visiting staff member at Los Alamos. Olle holds several awards, including the 1994 Prize for Young Researchers given by the Swedish government annually to "the best research work of the year." His interests lie in magnetism, electronic structure, f electron materials, theories of electron correlations, optical and magneto optical properties, as well as structural and cohesive properties of matter and their pressure dependence. He is currently professor in the Department of Physics, at the University of Uppsala.